Novel Adaptive Tone Reservation algorithm for PAPR reduction in massive Point-to-Point MIMO-OFDM systems

Author

Lalarukh Shairani

00000205609

Supervisor

Ass. Prof. Dr. Abdul Wakeel

Submitted to the Faculty of Department of Electrical Engineering
Military College of Signals, Rawalpindi
National University of Sciences and Technology, in partial fulfillment
for the requirements of MS Degree in Electrical Engineering (Telecommunication)
September 2021

Thesis Acceptance Certificate

Certified that final copy of MS/MPhil thesis written by Ms. **Lalarukh Shairani** of **MSEE-23 Course,** Registration No. **00000205609**, of **Military College of Signals** has been vetted by undersigned, found complete in all respect as per NUST Statutes/ Regulations, is free of plagiarism, errors, mistakes and, is accepted as partial fulfillment for the award of MS degree. It is further certified that necessary amendments as pointed out by GEC members of the student have been also incorporated in the said thesis.

Signature: _____

Name of Supervisor: Asst Prof. Dr. Abdul Wakeel

Date: _____

Signature (HoD): _____

Date: _____

Signature (Dean): _____

Date: _____

Dedication

To my family including my husband and in-laws.

Certificate

This is to certify that work in this thesis has been carried out by **Ms. Lalarukh Shairani** and completed under my supervision at Military College of Signals, National University of Sciences and Technology, Islamabad, Pakistan.

Supervisor: _____

Asst. Prof. Dr. Abdul Wakeel

MCS, NUST, Islamabad.

Acknowledgment

I am thankful to Allah Almighty for helping me achieve another milestone in my academics. Secondly, I want to thank the Military College of Signals, NUST, and the whole faculty for giving me a research environment at the institute. This would have not been possible without the support of my supervisor Asst. Prof. Dr. Abdul Wakeel, who not only provided timely guidance, profound encouragement and positive criticism but also ensured that I complete the assigned tasks in a defined time frame. His kind consideration helped me during all this time. I am also very obliged to my committee members, Dr. Alina Mirza and Dr. Mir Yasir Umair for their association with my work.

This would've not been possible without the support and prayers of my Parents, Husband and family.

Abstract

MIMO-OFDM is an emerging wireless technology that also covers the broadband aspect of communication. This technology has gained immense fame for its ability to adapt high-rate data transmission and robustness against multipath fading and other channel impairments. However, a major issue with a multicarrier system is their high peak-to-average ratio (PAPR) and, hence, massive MIMO-OFDM systems also suffer from high PAPR. Moreover, for massive MIMO-OFDM, where a large number of antennas are involved, the PAPR issue becomes more challenging. Different solutions have been proposed for PAPR reduction in MIMO-OFDM with some of them been extended to massive MIMO-OFDM systems; however, the proposed techniques have certain limitations, i.e., they are very complex.

Herein, we propose an adaptive Beam Reservation (BR) algorithm for PAPR reduction in P-to-P Massive MIMO-OFDM systems. Using Singular value decomposition (SVD) for a P-to-P MIMO-OFDM system, the channel matrix can be diagonalized into unitary matrices and a diagonal matrix containing singular values. It has been found out that the last singular values of a channel gain matrix are very weak such that these eigenchannels are ignored in the case of data transmission. In our proposal, the weakest eigen channel in our system is kept aside to offer redundancy for PAPR reduction. A spiky function is then generated on that weakest eigen channel, which is then used for PAPR reduction. Simulations results show that the proposed technique has promising gains in terms of PAPR reduction with a negligible increase in the mean power of the transmit signal and has a very low-capacity loss. Moreover, our proposed technique outperforms the conventional Tone Reservation algorithm in terms of PAPR reduction, mean power increase and capacity loss.

List of Contents

Thesis Acceptance Certificate i
Dedication ii
Certificate iii
Acknowledgment iv
Abstract v
List of Contents vi
List of Figures viii
List of Abbreviations xi
1. Chapter 1: 1
1.1. Multicarrier Systems 1
1.2. Orthogonal Frequency Division Multiplexing (OFDM) 2
1.2.1. Discrete-time OFDM 3
1.3. Multi-Antenna Systems 5
1.3.1. Multi Input Single Output (MISO) 6
1.3.2. Single Input Multiple Output (SIMO) 6
1.3.3. Point-to-Point MIMO 7
1.4. MIMO-OFDM system 9
1.5. OFDM based Massive MIMO 11
1.5.1. Massive MIMO 11
1.5.2. Potentials of Massive MIMO 12
1.5.3. Limiting Factors of Massive MIMO 13
1.6. PAPR of OFDM signal 13
1.7. Problem Statement 14
1.8. Proposed Solution 15
2. Chapter 2: 16
2.1. Peak to Average Power Ratio (PAPR) 16
2.1.1. Mathematical Expression 16
2.1.2. Statistical Analysis 18
2.2. PAPR Reduction Techniques in SISO Systems 19
2.2.1. Clipping 19
2.2.2. Selected Mapping 20

2.2.3. Partial Transmit Sequences 21
2.2.4. Tone Reservation 22
2.3. PAPR Reduction Techniques in MIMO Systems 23
2.3.1. Selected Mapping / Partial Transmit Sequences 24
2.3.2. Tone Reservation 24
2.3.3. Least Square (LS) 25
2.4. PAPR Reduction Techniques in Massive MIMO 25
2.4.1. BD-SLM 25
2.4.2. Simplified Iterative Discrete Estimations (SIDE) 26
2.4.3. ADMM approach 26
2.4.4. Clipping & Filtering 27
2.4.5. Adaptive Peak Cancellation 27
2.4.6. UBR 28
2.4.7. SDR based Approach 29
2.4.8. Enhanced Peak Cancellation 29
2.4.9. TR Algorithm 30
2.4.10. Machine Learning Approach 30
3. Chapter 3: 32
3.1. Adaptive BR Algorithm for PAPR Reduction in MIMO-OFDM Systems. 32
3.1.1. Key idea 33
3.1.2. System Model 34
3.1.3. A Spiky Function 36
3.2. Beam Reservation algorithm 36
3.3. Simulations 37
3.3.1. PAPR reduction using BR algorithm 39
3.3.2. Relative mean power increase ($\Delta \boldsymbol{E}$) 41
3.3.3. Capacity analysis of proposed BR algorithm 43
3.4. Conventional TR vs Proposed BR algorithm 44
3.4.1. PAPR reduction comparison 44
3.4.2. Performance comparison under mean power constraint 46
3.4.3. Capacity loss of CTR against our proposed BR algorithm 46
4. Chapter 4: 50
References 51

List of Figures

FIGURE 1.1 TRANSCEIVER STRUCTURE OF OFDM SYSTEM 4

FIGURE 1.2 MISO SYSTEM MODEL (UPLINK) 6

FIGURE 1.3 SIMO SYSTEM MODEL(DOWNLINK) 6

FIGURE 1.4 POINT TO POINT MIMO SYSTEM MODEL 7

FIGURE 1.5 BLOCK DIAGRAM OF A MIMO-OFDM TRANSMITTER SYSTEM MODEL 10

FIGURE 1.6 SIMPLE MASSIVE MIMO SYSTEM 12

FIGURE 1.7 DEPLOYMENT OF MASSIVE MIMO 12

FIGURE 2.1 BLOCK DIAGRAM OF SLM 21

FIGURE 2.2 BLOCK DIAGRAM FOR PTS 22

FIGURE 2.3 AN OFDM FRAME DEPICTING THE RESERVED TONES 22

FIGURE 2.4 SYSTEM MODEL OF THE MASSIVE MULTI-USER MIMO-OFDM DOWNLINK SCENARIO 27

FIGURE 2.5 THE MODIFIED C&F BLOCK 27

FIGURE 2.6 BLOCK DIAGRAM FOR MASSIVE MIMO SYSTEM DEPICTING PEAK CANCELLATION 28

FIGURE 2.7 BLOCK DIAGRAM OF THE PROPOSED METHOD 29

FIGURE 2.8 FUNCTIONAL WORKFLOW FOR PAPR REDUCTION 31

FIGURE 3.1 TRANSMITTER SYSTEM MODEL WITH BR ALGORITHM 34

FIGURE 3.2 USING SVD FOR THE DIAGONALIZATION OF MIMO CHANNEL 34

FIGURE 3.3 PAPR CURVES FOR A 10×10 MIMO-OFDM FOR THE PROPOSED BR ALGORITHM, WITH TARGET VALUE = 5.5 DB; WITH A COMBINED SEARCH ALGORITHM 39

FIGURE 3.4 PAPR CURVES FOR A 50×50 MASSIVE MIMO-OFDM FOR THE PROPOSED BR ALGORITHM, WITH TARGET VALUE = 5.5 DB; WITH A COMBINED SEARCH ALGORITHM 40

FIGURE 3.5 PAPR CURVES FOR A 10×10 MIMO-OFDM FOR THE PROPOSED BR ALGORITHM, WITH TARGET VALUE = 5.5 DB; WITH A COMBINED INDIVIDUAL ALGORITHM 40

FIGURE 3.6 PAPR CURVES FOR A 50×50 MASSIVE MIMO-OFDM FOR THE PROPOSED BR ALGORITHM, WITH TARGET VALUE = 5.5 DB; WITH A INDIVIDUAL SEARCH ALGORITHM..... 41

FIGURE 3.7 CCDF OF PROPOSED BR ALGORITHM WITH DIFFERENT MPC VALUES FOR 10×10 P-TO-P MIMO-OFDM, PAPR TARGET VALUE = 5.5DB, USING A COMBINED SEARCH ALGORITHM 42

FIGURE 3.8 CCDF OF PROPOSED BR ALGORITHM WITH DIFFERENT MPC VALUES FOR 50×50 P-TO-P MASSIVE MIMO-OFDM, PAPR TARGET VALUE = 5.5DB, USING A COMBINED SEARCH ALGORITHM 43

FIGURE 3.9 CHANNEL CAPACITY ANALYSIS FOR A P-TO-P 50×50 MASSIVE MIMO-OFDM SYSTEM UTILIZING BR ALGORITHM 43

FIGURE 3.10 CHANNEL CAPACITY ANALYSIS FOR A P-TO-P 50×50 MASSIVE MIMO-OFDM SYSTEM UTILIZING BR ALGORITHM WITH WATER-FILLING..... 44

FIGURE 3.11 CCDF(PAPR) COMPARISON OF A 10×10 MIMO-OFDM SYSTEM USING BR (BR) WITH A SYSTEM USING CTR WITH 10% RESERVED TONES 45

FIGURE 3.12 CCDF(PAPR) COMPARISON OF A 50×50 MASSIVE MIMO-OFDM SYSTEM USING BR WITH A SYSTEM USING CTR WITH 10% RESERVED TONES..... 45

FIGURE 3.13 CCDF FOR A 10×10 P-TO-P MIMO-OFDM SYSTEM, USING BR AND CTR ALGORITHMS UNDER A MEAN POWER CONSTRAINT 46

FIGURE 3.14 CAPACITY ANALYSIS FOR A P-TO-P 10×10 MIMO-OFDM SYSTEM UTILIZING BR WITH A SYSTEM USING CTR WITH DIFFERENT VALUES OF RESERVED TONES 47

FIGURE 3.15 CAPACITY ANALYSIS FOR A P-TO-P 10×10 MIMO-OFDM SYSTEM UTILIZING BR WITH A SYSTEM USING CTR WITH DIFFERENT VALUES OF RESERVED TONES WITH WATER-FILLING..... 48

FIGURE 3.16 CAPACITY ANALYSIS FOR A P-TO-P 50×50 MASSIVE MIMO-OFDM SYSTEM UTILIZING BR WITH A SYSTEM USING CTR WITH DIFFERENT VALUES OF RESERVED TONES..... 48

FIGURE 3.17 CAPACITY ANALYSIS FOR A P-TO-P 50×50 MASSIVE MIMO-OFDM SYSTEM UTILIZING BR WITH A SYSTEM USING CTR WITH DIFFERENT VALUES OF RESERVED TONES WITH WATER-FILLING 49

FIGURE 3.18 CAPACITY ASSOCIATED WITH LAST EIGENCHANNEL 49

List of Abbreviations

OFDM	Orthogonal Frequency Division Multiplexing
MIMO	Multiple input multiple output
SLM	Selected Level Mapping
PTS	Partial Transmit Sequence
BS	Base Station
i.i.d.	Independent Identically Distributed
CLT	Central Limit Theorem
PAPR	Peak to Average Power Ratio
TR	Tone Reservation
PA	Power Amplifier
BER	Bit Error Rate
OOB	Out Of Band radiation
SOCP	Second Order Cone Programming
BD	Block Diagonal

Chapter 1:
Introduction

Data communication has become an essential part of our life. Phone calls (audio/video), texting, live streaming, downloading of content (documents/ audios/ videos), social websites, and applications have become a necessary part of our life. Different softwares and applications like Skype, WhatsApp, and Teams, e.t.c., are being used for arranging meetings, classes, social calls, and many other purposes. With this ever-increasing development in technology and the increasing number of consumers, the demand for high and reliable data transmission rates is difficult to meet if we use the older transmission systems. Wired systems were a novel way to communicate when they were introduced but with the introduction of wireless and the internet, we have seen a huge evolution in our daily life. However, it is not like the wireless system is error-free or noise-free as our wireless medium is filled with obstacles that affect the signal. Channel fading, inter symbol interference (ISI), and channel noise are a few of the major challenges that we face in wireless communication.

In this chapter, we start with Orthogonal Frequency Division Multiplexing (OFDM) one of the most popular multicarrier techniques in Sections 1.1 and 1.2. Section 1.3 will be an introduction to the multi-antenna system and a brief discussion of its variants. Section 1.4 will give a look into the working of MIMO-OFDM systems. The overview of Massive MIMO, its advantages and limitations are deliberated in section 1.5. Section 1.6 will discuss the Peak to average power ratio (PAPR) of the OFDM system and its negative effects, which extend into the MIMO systems and the problem statement is delivered in section 1.7. Our proposed solution is briefly touched upon in section 1.8.

1.1. Multicarrier Systems

Multicarrier modulation is done by dividing the data that is to be transmitted into multiple chunks and then sending each of these individual chunks over different

carrier frequencies. The individual carrier signals have small bandwidth, but the signal obtained after combining these individual carriers can have broad bandwidth.

1.2. Orthogonal Frequency Division Multiplexing (OFDM)

OFDM is one of the most commonly used multicarrier modulation techniques which is known for its flexibility and ease of implementation. It is known for its robust and reliable transmission of high data rates across noisy channels.

OFDM divides a wideband channel into orthogonal narrowband subchannels, that are ideally independent of each other. OFDM is an orthogonal subcarrier variant of Frequency Division Multiplexing (FDM). It has gained a good reputation in modern communication systems over the last 20-30 years, but the concept of OFDM dates back to the mid-1960s.

The concept was first introduced in 1966 by Chang in [1]. Saltzberg extended Chang's principle by integrating the multicarrier systems with Offset Quadrature Amplitude Modulation (OQAM) in [2].

In [3], Weinstein and Ebert proposed to use DFT for the modulation of OFDM signal at transmitter's side and demodulation of it at receiver's side in [3]; thus, reducing the intricacy of the system. The use of Fast Fourier Transform (FFT) further reduced the system's complexity from N^2 operations to $\left(\frac{N}{2}\right)\log N$ operations [4].

In 1980, Peled and Ruiz proposed to fill the empty guard space between two successive OFDM frames with a cyclic extension (CP); thereby resolving multipath channels issue of lack of orthogonality [5].

Hirosaki proposed an orthogonally multiplexed QAM system with an equalization technique that is based on a sub-channel approach to remove inter-symbol interference (ISI) and crosstalk for OQAM-OFDM systems in 1980 [6]. Later in 1980, he introduced the OFDM system with DFT-based implementations [7].

In [8], Alard et al used OFDM technique for the broadcasting purpose in consideration of mobile users. In the last 20 years, the use of OFDM in practical systems has increased dramatically i.e, ADSL, VHDSL, WLANs, etc.

1.2.1. Discrete-time OFDM

In OFDM, a wideband channel is partitioned into parallel subchannels working at different frequencies in multicarrier modulation [9] and [10]. A number of channels are decided so that the bandwidth of sub-channels $\mathbf{W_N}$ is less than the coherence bandwidth W_c to minimize ISI [9]. OFDM implementation allows the frequency spectrum to overlap; which results in a more efficient utilization of bandwidth.

The computational complexity of the multicarrier system is greater as compared to the conventional single-carrier systems. The previous systems were complex as they require required a **N** number of modulators, transmit filters, demodulators and receive filters for **N** number of sub-channels. So with the increasing number of sub-channels, the number of modulators, demodulators and filters also increased linearly. Thus, increasing the computational complexity of the multicarrier system.

The issue of complexity was somewhat diminished by using DFT and IDFT [3] on a signal so that we can transform the signal's domain from time to frequency and vice versa, respectively. The IDFT of a data stream (**A = [A_n]**, and n = 1, 2, . . ., N) in frequency domain is obtained by using

$$[\boldsymbol{a_k}] = \text{IDFT}[\boldsymbol{A_N}] = \frac{1}{\sqrt{N}}\sum_{n=1}^{N} \boldsymbol{A_n} e^{j\frac{2\pi nk}{N}}, 1 \leq k \leq N, \quad (1.3)$$

where $\mathbf{a_k}$ is the k^{th} sample of the sequence in discrete time **(a = [a_k]),** and N is that sample's frame size. The information sequence **[A_n]** that is in the frequency domain can be recovered by using the DFT (Fast Fourier Transform (FFT)) function over the discrete-time sequence **[a_k]** given as,

$$[\boldsymbol{A_n}] = \text{DFT}[\boldsymbol{a_k}] = \frac{1}{\sqrt{N}}\sum_{n=1}^{N} \boldsymbol{a_k} e^{-j\frac{2\pi nk}{N}}, \text{ where } 1 \leq n \leq N, \quad (1.4)$$

The DFT modulator correlates the input signal with the sinusoidal basic functions that cause peak at a certain frequency; while the energy of other sub-carriers is nullified at that frequency [10].

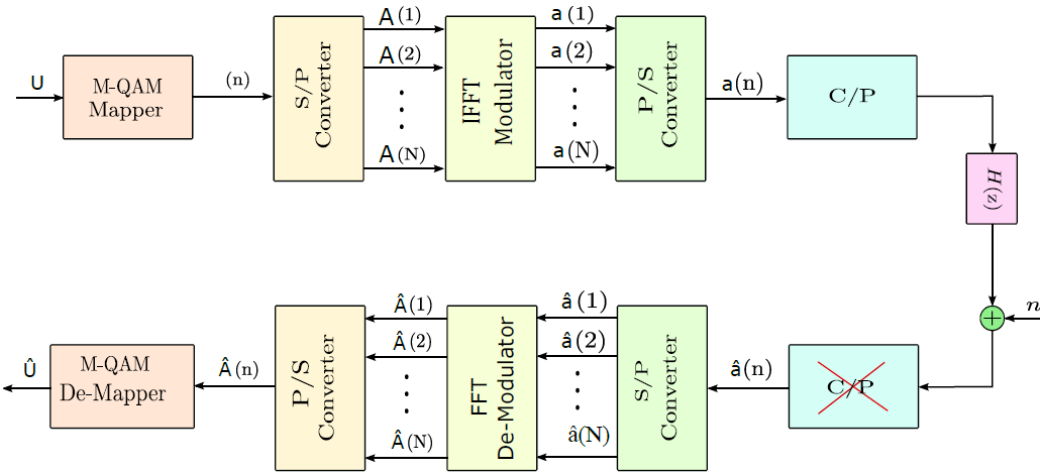

Figure 1.1 Transceiver structure of OFDM system

A block diagram of an OFDM system that uses DFT is shown in Fig 1.1. The information bits **U** are transformed to *N* QAM symbols. These symbols (**A=[A$_n$]**, n = 1, 2, . . ., N) are sent over each subcarrier channel. These symbols **A$_n$** are complex numbers (i.e., **A$_n$** = **A$_U$**(n) + *j***A$_Q$** (n)), that represents a M-*ARY* QAM constellation with as

$$\boldsymbol{A_n} \in \{\pm \boldsymbol{A_U}(n) \pm j\boldsymbol{A_Q}(n)\}, \text{ where } \quad \boldsymbol{A_{U/Q}}(n) \in \left\{\frac{1}{2}, \frac{3}{2}, \ldots, \frac{\sqrt{3}-1}{2}\right\} \quad (1.5)$$

Only data rates and channel properties can be used to select the M-*ARY* QAM constellation. The serial QAM symbols [**A$_n$**] are then changed to parallel stream ([**A$_n$**], i.e., [**A$_n$**]→**[A$_n$]^T**, where T represents transpose function) after passing from a serial to parallel converter (S/P). IDFT (IFFT) modulator transforms the frequency domain OFDM symbol to the time domain symbol.

A parallel-to-serial (P/S) converter is utilized after that to convert the parallel time-domain stream into a serial one. The serial data stream is then appended in the time domain, with a periodic extension of the OFDM signal, known as Cyclic Prefix (CP).

The resulting OFDM frame is then sent over a noisy channel after attaching the CP to the stream. The impulse response of that channel is **H(z)**.

At the receiver terminal, firstly the CP is separated from the received signal [$\hat{\mathbf{a}}_k$] and then converted to a parallel stream by utilizing an S/P converter. Then, the received time-domain signal is converted into a frequency-domain signal by going through the DFT modulator. By utilizing a frequency domain equalizer, the received symbols are de-mapped.

Modern communications systems are attempting to utilize the other available properties of signals such as space and time, in addition to the available spectrum. One of the most popular methods available is Multiple Input Multiple Output (MIMO) transmission.

1.3. Multi-Antenna Systems

MIMO is one of the key technologies of LTE-A. It is a system with multiple antennas on the transmitter and/or receiver. This type of multiple-antenna system can boost system performance in many dimensions and have the capability to challenge Shannon limit [11] by increasing throughput many folds and giving cutting edge advantages in diversity, multiplexing, array gains and interference reduction. These antennas can give diversity gain which tends to make improvements in the BER performance, improvement of system's capacity by the virtue of multiplexing gain; and by reducing the interference in the spatial domain via utilizing the directivity gain from multiple antennas. The demand for high data rates has led us to the use of multi-antennas at the transmit and receive terminals; thus, forming the Multiple-antenna (MA) system.

The multi-antenna systems are divided into three categories according to their deployment scenarios,

a) Multiple Input Single Output (MISO)

b) Single Input Multiple Output (SIMO)

c) Multiple Input Multiple Output (MIMO)

1.3.1. Multi Input Single Output (MISO)

A MISO system, as shown in Fig 1.2, has T independent users with variable number of antennas at their transmitting terminals, communicates with a central base station (BS) having multiple antennas. The central BS is acting as a receiver to the individual users, so, we will consider the post-processing at the receiver side. As a large number of users communicate with the Base Station (BS), this scenario is also called Multiple Access Channel (MAC).

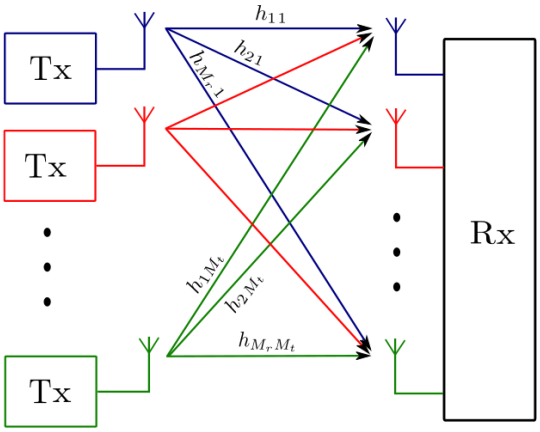

Figure 1.2 MISO system model (uplink)

1.3.2. Single Input Multiple Output (SIMO)

Figure 1.3 shows a downlink scenario, the information is transmitted from the BS to the multiple mobile users, which is why this scenario is also known as the broadcast channel (BC). The pre-processing or pre-coding is considered at the central BS.

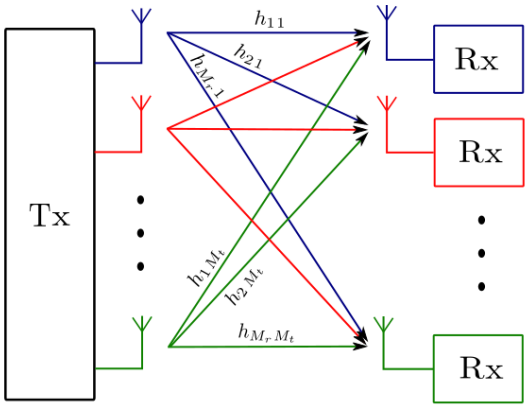

Figure 1.3 SIMO system model(downlink)

1.3.3. Point-to-Point MIMO

For P-to-P setups, signal processing is probable at both ends, the transmitter and the receiver terminals. In Fig 1.4, we assume a single user P-to-P MIMO system having an identical number of transmit and receive antennas, i.e., $\mathbf{M_t = M_r}$. With the consideration of perfect CSI at the transmitter, precoding (pre-processing) is done at the transmitter terminal and post-processing of the received data is done at receiver terminal.

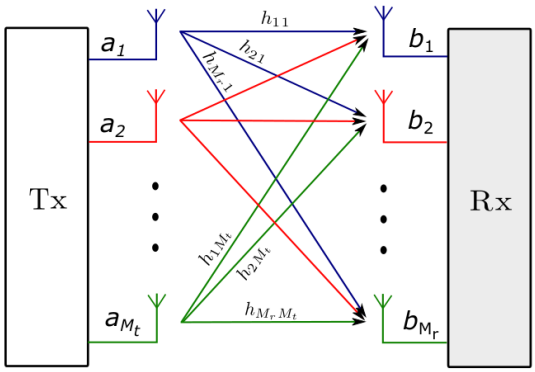

Figure 1.4 Point to Point MIMO system model

P-to-P MIMO System Model

Consider a P-to-P MIMO system having M_t and M_r antennas at transmitter and receiver terminals, respectively. Assume that the input data to the MIMO system is $\mathbf{A = [A_t] = [A_1, A_2, \ldots, A_{M_t}]^T}$; where $\boldsymbol{A}$ is the transmitted data that passes through the MIMO channel. The received vector $\mathbf{B = [B_r] = [B_1, B_2, \ldots, B_{M_r}]^T}$ at the receiver side is written in matrix form as

$$\begin{pmatrix} B_1 \\ B_2 \\ \vdots \\ B_{Mr} \end{pmatrix} = \begin{pmatrix} h_{1\,1} & h_{1\,2} & \ldots & h_{1\,Mt} \\ h_{2\,1} & h_{2\,2} & \ldots & h_{1\,Mt} \\ \vdots & \vdots & \ddots & \vdots \\ h_{Mr\,1} & h_{Mr\,2} & \ldots & h_{Mr\,Mt} \end{pmatrix} \begin{pmatrix} A_1 \\ A_2 \\ \vdots \\ A_{Mt} \end{pmatrix} + \begin{pmatrix} \mathrm{W}_1 \\ \mathrm{W}_2 \\ \vdots \\ \mathrm{W}_{Mr} \end{pmatrix} \qquad (1.6)$$

In compact form, we write

$$\mathbf{B = HA + W}, \qquad (1.7)$$

where **H** is the $\mathbf{M_r \times M_t}$ channel gain matrix and its coefficients are the results from the relation between the different transmit to the receive antenna. The **A, B** and **W** are column vectors where **W** is the zero mean additive white Gaussian noise variance defined by $\boldsymbol{\sigma_r^2}$. By applying singular value decomposition (**SVD**), we get the following equation

$$\mathbf{H = C\ \Delta\ E}^{\mathrm{H}} \tag{1.8}$$

H is the channel gain matrix. **C** and **E** are the unitary matrices such that the relation $\mathbf{C^H\ C = E^H\ E = I}$ holds. **Δ** is a diagonal matrix having rank $\mathbf{R_H \leq}$ min ($\mathbf{M_r\ M_t}$) and its singular values ($\boldsymbol{\delta_{ij}} = \mathbf{[\delta_{11}, \delta_{22}, \ldots, \delta_{R_H R_H}, 0, \ldots, 0]}$) are obtained from **H**. These values are normally arranged in a descending manner, i.e, $\boldsymbol{\delta_{11} \geq \delta_{22} \geq \ldots \geq \delta_{R_H R_H}}$.

Considering a P-to-P MIMO system (having perfect CSI), the diagonalization of the channel matrix **H** is done by multiplying pre-processing matrix **E** with input data vector, i.e., $\mathbf{A = E\ \tilde{A}}$. The post-processing of the received signal is done at the receiver side by the post-processing matrix $\mathbf{C^H}$, i.e.,

$$\mathbf{\tilde{B} = C^H B = C^H (H\ A + W)} \tag{1.9}$$

Herewith, Eq. (1.9) is reformed as

$$\mathbf{\tilde{B}} = \mathbf{C^H}.\mathbf{C}.\Delta.\mathbf{E^H}.\mathbf{E}.\mathbf{\tilde{A}} + \mathbf{C^H W} \tag{1.10}$$

which simplifies to

$$\mathbf{\tilde{B}} = \Delta.\mathbf{A} + \mathbf{\tilde{W}} \tag{1.11}$$

Here, Δ is the diagonalization matrix of **H** containing the values $\boldsymbol{\delta_k}$ and $\mathbf{\tilde{W}}$ is the noise vector. For an **M×M** channel matrix, neglecting the noise vector, Eq. (1.11) in matrix form becomes

$$\begin{pmatrix} \tilde{B}_1 \\ \tilde{B}_2 \\ \vdots \\ \tilde{B}_M \end{pmatrix} = \begin{pmatrix} \delta_{1,1} & 0 & 0 & 0 \\ 0 & \delta_{2,2} & 0 & 0 \\ 0 & 0 & \ddots & 0 \\ 0 & 0 & 0 & \delta_{M,M} \end{pmatrix} \begin{pmatrix} \tilde{A}_1 \\ \tilde{A}_2 \\ \vdots \\ \tilde{A}_M \end{pmatrix} \tag{1.12}$$

Where $\boldsymbol{\delta_{1,1}, \delta_{2,2}, \ldots, \delta_{M,M}}$ are the gains of the eigenchannels.

1.4. MIMO-OFDM system

In the era stormed with wireless consumers soliciting for enhanced data rate coupled with reliability, MIMO-OFDM is an emerging wireless technology that also covers the broadband aspect of communication. This technology has gained immense fame for its ability to adapt high-rate data transmission and robustness against multipath fading and other channel's diminishing effects. Here, the term MIMO-OFDM is used to address only OFDM as the multiplexing technique, combined with multiple antennas in a wireless link. A major issue that was raised in MIMO-OFDM systems is the ability to acquire perfect CSI followed by prompt coherent detection required for information symbols and channel synchronization. However, OFDM gives a fractional solution to spectral efficiency unless augmented by MIMO. In 1990, authors namely Foschini and Gans in [12] and Telatar in [13] claimed to show an alternative way of attaining a high data rate by utilizing multiple antennas. This approach was named as MA (multiple antenna) system and later termed as MIMO in [12][13].

The MIMO technique utilizes the same bandwidth and transmission power. The studies not only claimed but later proved to have enhanced spectral efficiency. Telatar in his paper [13] showed that in any given wireless system using transmit antennas $\mathbf{M_t}$ and receiving antennas $\mathbf{M_r}$, the maximum data rate that can be achieved in a fading channel is proportional to $\mathbf{M_t \times M_r}$. The condition applied for the fulfillment of this assumption is directly proportional to the availability of statistically independent channels between transmitter and receiver. This methodology explored a new approach namely the spatial domain, as compared to the time and frequency domains. The availability of a greater number of channels did not only provide high throughput gains but also provides adaptable environments in which data can be sent across the fading channel. Therefore, MIMO-OFDM is a safe bet for enhanced data rates in fixed and mobile communication. It is thus an auspicious technique for present communication systems, providing high data rates while ensuring reliable transmission. A block diagram of a general transceiver model of a P-to-P MIMO-OFDM system is shown in Fig 1.5.

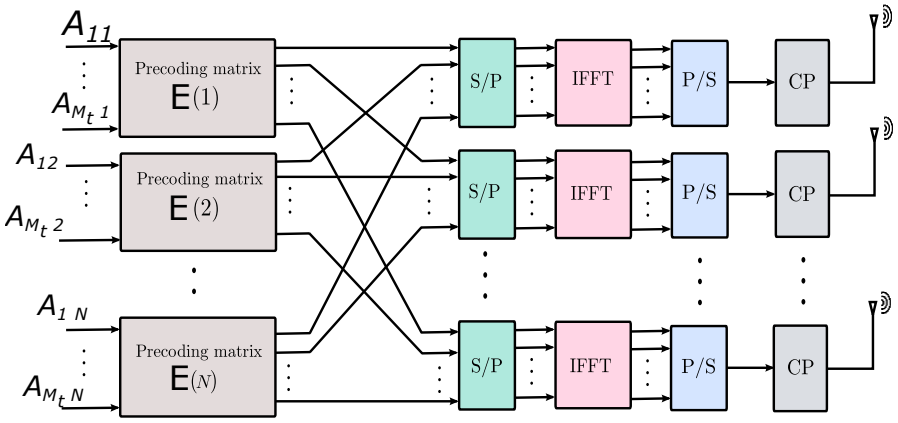

Figure 1.5 Block diagram of a MIMO-OFDM transmitter system model

With the assumption that $\boldsymbol{M_t = M_r = M}$ and **A(n)** is theinput vector. At the transmitter side precoding is done on the input vector **A = [A(1), A(2), · · · , A(N)]** by using pre-processing matrices **E = [E(1), E(2), . . ., E(N)]**. By using serial to parallel converter, they are transformed to a parallel data stream. After passing through the IFFT modulator, the resultant signal ***a*** **= [*a*(1) *a*(2) . . . *a*(N)]** is transformed into a time-domain and then it is appended with a cyclic extension called cyclic prefix, to lessen the effects of ISI. The appended signal is then sent over the channel with a channel matrix. On the receiver side, the opposite process is performed to get an approximation of the transmit signal. We name **b(n)** to be the output vector. The input signal **A(n)** is pre-processed by **E(n)** before performing IFFT, while the signal at the receiver terminal is post-processed by using $\mathbf{C^H(n)}$ after performing the FFT to obtain the estimated signal **B(n)**. The received symbol can be written as[14][15].

$$y_\mu = \sum_{j=1}^{M} h_{\mu,j}(n)a_j(n) + \mathrm{W}_\mu(n), \quad \mu = 1,\ 2,\ \ldots, M \tag{1.13}$$

Here a_j (n) is the input symbol whereas W_μ (n) represents the AWGN at receive antenna and $\mathbf{h}_{\mu,\,j}$ shows the channel coefficients. Then, the received data vector **b(*n*)** can be estimated as

$$\mathrm{b}(n) = \mathrm{H}(n)a(n) + \mathrm{W}(n) \tag{1.14}$$

where $\mathbf{W}(\boldsymbol{n})$ = [$\mathbf{W_1}(\boldsymbol{n}), \mathbf{W_2}(\boldsymbol{n}), \ldots, \mathbf{W_M}(\boldsymbol{n})]^{\mathbf{T}}$ is the Gaussian noise and $\mathbf{H}(\boldsymbol{n})$ is a channel gain matrix of dimension **M** × **M**. The MIMO-OFDM system's relationship between its input and output can be expressed as

$$B = HA + N \quad (1.15)$$

where B is the received vector of dimension $\mathbf{M_r\ N \times 1}$, **A** is the to be the transmit vector of dimension $\mathbf{M_t\ N \times 1}$, **H** is the channel gain matrix of dimension $\boldsymbol{M_r\ N \times M_t\ N}$ and **N** is AWGN vector of dimension $\mathbf{M_r\ N \times 1}$.

1.5. OFDM based Massive MIMO

Challenges are an essential part of research and development. The new developments are always towards the realization of the new user's needs and the boosts towards the quality of data communication and new services. From **1G** to **4G**, for every generation, a new key point index and services are defined and are attached and aroma of a generation. e.g., 1G was known as the age of Analogue communication, 2G as the age of Digital communication, in 3G we addressed the pseudorandom codes and 4G introduced us with the multi-carrier frequencies. The newest generation 5G will deal with the areas that were not covered by the previous generations. The 5G will introduce more spectral efficiency, higher data rates, efficient battery-consuming communication, increased capacity for users, low spectrum leakage and much more. OFDM-based Massive MIMO is a running candidate for the 5G technology with its inherent advantages from both the OFDM and MIMO technology.

1.5.1. Massive MIMO

Massive MIMO is an emerging technology, which is maturing with passage of time and is now being incorporated in Wi-Fi and LTE. Massive MIMO incorporates hundreds of antennas at BS and tens of antennas at MS, thereby the ordinary MIMO is being scaled up by many times higher. Massive MIMO is also named Large-Scale MIMO, Full dimension MIMO and ARGOS [16][17]. It uses the same frequency and time resources, but it has proved to have improved throughput, goodput and energy efficiency as well. The Massive MIMO was initially proposed for time-division duplexing but now, frequency division duplexing has also been chipped in for enhanced usage. Fig 1.6 below shows a simple Massive MIMO system.

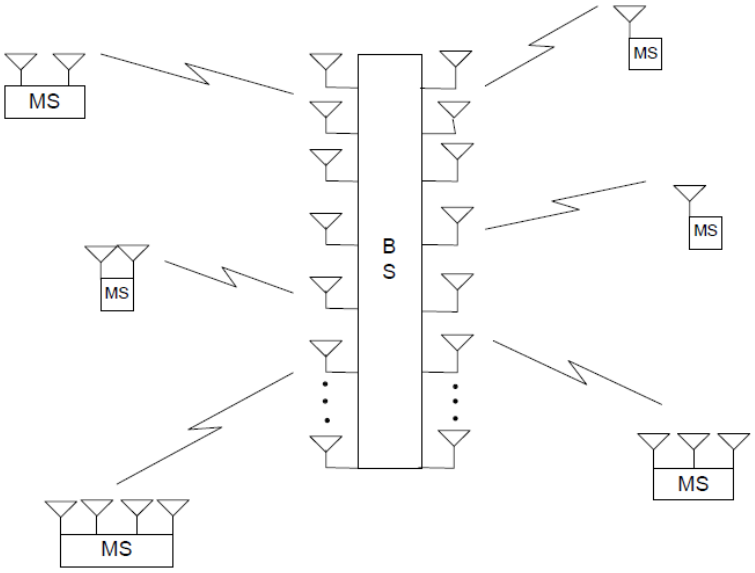

Figure 1.6 Simple Massive MIMO system

Principally, CSI is required at the transmitter as well as receiver in Massive MIMO. Figure 1.7 shows deployment options of the Massive MIMO system.

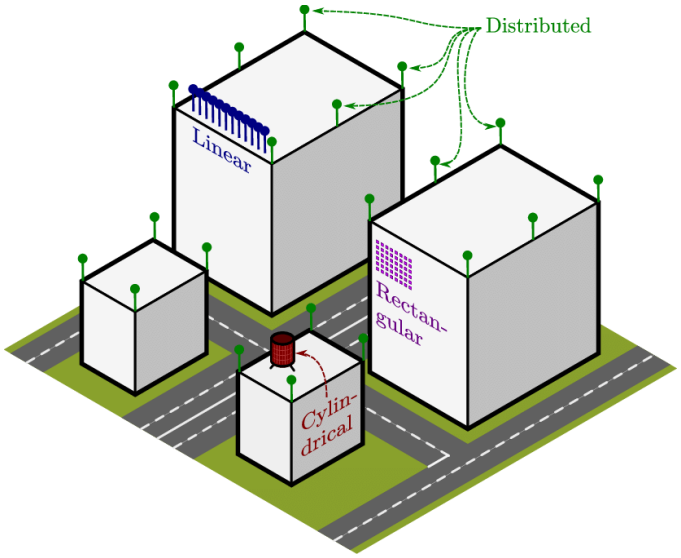

Figure 1.7 Deployment of Massive MIMO

1.5.2. Potentials of Massive MIMO

Some benefits of Massive MIMO are enumerated:

1. With an increased number of antennas, the capacity of the system can be enhanced to more than ten times, still, radiated energy efficiency is restricted to the order of almost the number of BS antennas.
2. As compared to simple MIMO, spectral efficiency is enhanced to an order of ten times. It is possible to use the same frequency and time resources for the support of multiple users at the same time.
3. The concept of Massive MIMO can be realized by using low-power and inexpensive components, thereby reducing the cost.
4. Extra antennas help to focus the energy and therefore ensure good reception in limited spaces.
5. Robustness against jamming and interference.

1.5.3. Limiting Factors of Massive MIMO

A few limitations of Massive MIMO include employment of low expense components causing calibration errors and resultantly inducing CSI difference. This limitation can be addressed with the increased complexity of the hardware. Next is a communication pillar of Massive MIMO, which is importance of independent and orthogonal channel response by all channels, as correlation in channels can prove to be very harmful. Another one is the high PAPR because of a large number of antennas involved in data transmission.

1.6. PAPR of OFDM signal

There are several reasons why OFDM is gaining popularity in modern communication systems, mainly owing to its advantages such as lower to no ISI, its ability to be easily implemented with the usage of DFT and IDFT modulators and the optimum use of the spectrum alongside the use of overlapping orthogonal subcarriers. One major disadvantage of the OFDM system is **Peak-to-Average Power (PAPR) ratio**, that is the transmit signals have a high dynamic range.

Peak-to-Average power ratio (PAPR) is a term coined for the difference between peak power and average power of an OFDM signal, defined as

$$\text{PAPR}\,(a) = \frac{\max\limits_{k,1\leq k\leq N} |a_k|^2}{E\{|a_k|^2\}} \tag{1.16}$$

The envelope's maximum peak power amplitude is represented by $max_k|x_k|^2$ and the average power over of an OFDM symbol is denoted by $E\{|a_k|^2\}$.

1.7. Problem Statement

OFDM systems provide many advantages for our communication systems but their foremost shortcoming is its high peak to average power ratio (PAPR). As the QAM symbols are i.i.d., then according to the Central Limit Theorem (CLT), they may lead to a Gaussian-like distribution and constructively add up on some occasions. As a result, there is a drastic change between peak power of the signals in the time domain and its average power. The higher power efficiency of the non-linear devices like amplifiers entails them to be operated in the linear region. In the case of single-carrier systems, the operating point in the amplifier can be determined precisely without vicious nonlinear impairments. However, in the case of multi-carrier systems, time-domain signals have a sporadic peak. Such a signal will drive the power amplifiers to operate in their non-linear region, which will result in signal clipping. Signal clipping will result in in-band distortion and out-of-band radiation. The in-band distortion results in high Bit Error Rates (BER).

Moreover, due to out-of-band radiation (OOB), subcarriers are no more orthogonal that causes crosstalk. The signal becomes sensitive to non-linearity so it is required to measure the signal to show how much it is sensitive to non-linearity.

Therefore, countermeasures are required to be taken to stop the power amplifiers from operating in their non-linear regions. An eminent measure for the multi-carrier signals is PAPR [18]. Fluctuation in the signal depends on the PAPR i.e., the higher the PAPR, more will be the fluctuations. As a result of this, the operating point in the amplifier needs to be set at a higher point away from the saturation point using high power back-ups, which results in inefficient use of power.

An OFDM signal is comprised of several independent subcarriers that give a large PAPR when added up constructively. This addition gives high peak power however keeping the mean power low. Signals with same phase, when added give the highest PAPR; so, there is a need to reduce this high PAPR [18].

Moreover, MIMO-OFDM systems inherit this issue from OFDM. Moreover, for MIMO-OFDM the PAPR becomes a difficult task due to the high number of

antennas. Similarly, for Massive MIMO-OFDM systems, that involve a massive number of antennas, this issue becomes more challenging.

1.8. Proposed Solution

Many PAPR reduction techniques have been introduced and modified over the last few decades. In our approach, we propose a novel adaptive **Beam Reservation (BR)** algorithm for PAPR reduction in p-to-p massive MIMO-OFDM systems. In **BR** algorithm, the weakest Eigen channels is reserved for PAPR reduction. A specifically designed spiky function is then generated on that weakest Eigen channel, which is then iteratively added (or subtracted) to the transmit signal to reduce its PAPR. Its overall effectiveness is graded by observing its performance against conventional TR algorithm in Massive MIMO-OFDM by evaluating its performance via parameters like PAPR reduction, performance under different mean power constraints and capacity analysis.

Chapter 2:

Literature Review

Chapter 1 dealt with a short introduction of the multicarrier system (but focused on one of its types i.e., OFDM), multi-antenna systems and its types, OFDM based MIMO systems, Massive MIMO systems and one of the most popular criteria to judge a system's performance is the peak to average power ratio (PAPR) of that system. The previous chapter also deals with the explanation of disadvantages we face with high PAPR, which takes us to our main issue in this literature.

We will start this chapter by again shortly stating the PAPR definition, its mathematical expression and its statistical analysis. In section 2.2, we will state some of the most popular techniques that are being used for SISO systems that can be extended in the case of OFDM based MIMO systems. The techniques used for PAPR reduction in MIMO systems are listed in section 2.3 and section 2.4 deals with the PAPR reduction techniques that are being used for Massive MIMO.

2.1. Peak to Average Power Ratio (PAPR)

PAPR is the ratio of the maximum power to the average power of the transmitted OFDM symbol [19], defined as

$$\mathrm{PAPR}(a) = \frac{\max_{k,1\leq k\leq N} |a_k|^2}{E\{|a_k|^2\}} \tag{2.1}$$

2.1.1. Mathematical Expression

Let $\boldsymbol{A} = [A_n], 1 \leq n \leq N$, be the input QAM symbols vector. Applying IFFT on the frequency domain signal, we get$a = [a_k], 1 \leq k \leq N$in time domain.

$$a_k = \frac{1}{\sqrt{N}} \sum_{n=1}^{N} A_n \, e^{j\frac{2\pi nk}{N}} \tag{2.2}$$

In the case of the OFDM system where there are *N* subcarriers, the power $|a_k|^2$of the time domain transmit signal *a* at an instant is

$$|a_k|^2 = a_k a_k^* = \frac{1}{\sqrt{N}}\sum_{n=1}^{N} A_n\, e^{j\frac{2\pi nk}{N}} \cdot \frac{1}{\sqrt{N}}\sum_{m=1}^{N} A_m\, e^{j\frac{2\pi mk}{N}} \tag{2.3}$$

By applying Euler formulas, it can be simplified as

$$|a_k|^2 = \frac{1}{N}\left\{\sum_{n=1}^{N}|A_n|^2 + \sum_{n=1}^{N}\sum_{n\neq m} A_n A_m e^{j\frac{2\pi k(n-m)}{N}}\right\} \tag{2.4}$$

The average power of a time-domain signal relates to power in the DFT domain is written by using Parseval's theorem as

$$E\{|a_k|^2\} = E\{|A_n|^2\} \tag{2.5}$$

The peak power of an OFDM signal can be simplified [20] by using Eq 2.5 as

$$\begin{aligned}
\max_k |a_k|^2 &= \frac{1}{N}\max_n \left\{\sum_{n=1}^{N}|A_n|^2 + \sum_{n=1}^{N}\sum_{n\neq m} A_n A_m e^{j\frac{2\pi k(n-m)}{N}}\right\} \\
&\leq \frac{1}{N}\left\{\max_n \sum_{n=1}^{N}|A_n|^2 + \max_n \sum_{n=1}^{N}\sum_{n\neq m} A_n A_m e^{j\frac{2\pi k(n-m)}{N}}\right\} \\
&\leq \frac{1}{N}\left\{N\max_n|A_n|^2 + N(N-1)\max_n|A_n|^2\right\} \\
&\leq \frac{1}{N}\left\{N^2\max_n|A_n|^2\right\} \\
&\leq \left\{N\max_n|A_n|^2\right\}
\end{aligned} \tag{2.6}$$

Using Eq 2.5 and 2.6, the PAPR in Eq 2.3 can be calculated as

$$\text{PAPR}\,(a) \leq N\frac{\max_{1\leq n\leq N}|A_n|^2}{E\{|A_n|^2\}} \tag{2.7}$$

If the phase is same for all the QAM symbols that were mapped from the *M-ARY* constellation, then the inequality in Eq2.7 is converted to equality and PAPR calculated in that case is the maximum, defined as

$$\text{PAPR}_{max}(a) = N\frac{\max_{1\le n\le N}|A_n|^2}{E\{|A_n|^2\}} \quad (2.8)$$

From Eq2.8, we deduce that the PAPR rises linearly with the rise in the number of sub-carriers (tones). Eq 2.8gives us the maximum limit of an OFDM symbol PAPR. In practice, the chance to get this is very little. As a result, the system's performance is judged by the statistical analysis of the PAPR of OFDM system.

2.1.2. Statistical Analysis

A statistical comparison of different PAPR reduction schemes is conducted by using the **Complemental Cumulative distribution function** (**CCDF**). The CCDF of the PAPR states the possibility for the PAPR to be higher than the threshold τ of an OFDM system, i.e., CCDF (PAPR) = P_r (PAPR $> \tau$).

For a large number of subcarriers, the power at an instant is $|\boldsymbol{a_k}|^2$. The Rayleigh distribution is formed, by taking the square root of the amplitude of the envelope of the OFDM symbols $\boldsymbol{a_k}$ that signifies the power, with a **Probability Density Function** (**pdf**) given as

$$pdf(a_k) = 2a_k e^{-|a_k|^2} \quad (2.9)$$

Let $\boldsymbol{\tau_k}$ be defined as the PAPR of the kth sample, then the statistical likelihood of the PAPR being smaller than the predefined threshold value τ is

$$CCDF_{\tau_k}(\tau) = \int_0^\tau pdf(\tau_k)d(\tau_k) = \int_0^\tau 2\tau_k e^{-|\tau_k|^2} d(\tau_k) = 1 - e^{-\tau} \therefore \tau_k \le \tau \quad (2.10)$$

The CCDF of an OFDM envelope with i.i.d. data samples $\boldsymbol{N}$ can then be written

$$CCDF_\tau(\tau) = \left(CCDF_{\tau_k}(\tau)\right)^N = (1 - e^{-\tau})^N \quad (2.11)$$

Using Eq 2.11, the CCDF is calculated as

$$CCDF(PAPR) = P_r(PAPR > \tau) = 1 - (1 - e^{-\tau})^N \quad (2.12)$$

The CCDF for a single-antenna OFDM system operating at the Nyquist rate is given by Eq 2.12. The application of statistical analysis to multi-antenna systems is simple. $\mathbf{M_t}$ OFDM frames are transmitted simultaneously in a multi-antenna system

having $\mathbf{M_t}$ transmit antennas. All these $\boldsymbol{M_t}$ OFDM frames are statistically independent at the input of all transmit antennas. So, there are $\boldsymbol{M_t N}$ samples in a multi-antenna situation. CCDF for MIMO-OFDM system having transmitter antennas $\boldsymbol{M_t}$ is

$$CCDF\ (PAPR) = (CCDF_{\tau_k}(\tau))^{M_t N} = (1 - e^{-\tau})^{M_t N} \tag{2.13}$$

Using Eq 2.14, we can formulate CCDF as

$$CCDF\ (PAPR) = 1 - (1 - e^{-\tau})^{M_t N} \tag{2.14}$$

2.2. PAPR Reduction Techniques in SISO Systems

The discussion so far has covered how all electronic devices, especially HPAs are power-limited. The amplifier is driven to operate in its non-linear region if we pass an OFDM signal whose peak value is higher than that of amplifier's operational range through the HPA. System performance is degraded owing to signal distortion caused by this process. Therefore, in order to bring peak values of the signal below the amplifier's linear operational range, steps are taken. In order to lower the peak excursion of an OFDM signal, various techniques have been proposed. Single-input single-output (SISO) systems were the first technology for which these techniques were proposed. Out of these proposed techniques, some have been extended for the PAPR reduction of multi-antenna systems. Let us begin with the discussion on the techniques introduced for SISO systems.

2.2.1. Clipping

The widely used simplest PAR reduction technique is Clipping. In this process, the D/A converter or HPA itself clips the peak excursions past a pre-determined threshold value of the HPA linear range. Mathematically, clipping can be expressed [21]–[28] as

$$a^c = \begin{cases} a & , \quad |a| \le \alpha_o \\ \alpha_o e^{j\ arg\{a\}}, & |a| > \alpha_o \end{cases} \tag{2.15}$$

In Eq 2.15, $\boldsymbol{a^c}$ is the clipped signal, $\mathbf{arg\{}\boldsymbol{a}\mathbf{\}}$ represents the phase of complex value $\boldsymbol{a}$ and $\boldsymbol{\alpha_o}$ is the pre-determined threshold value.

The transmitter is where clipping is done. The occurrence and distribution of high peaks are random. Hence, when we clip the signals, in-band distortion is the outcome which in turn give rise to the BER at the receiver and out-of-band radiations. Interference in adjacent bands is caused by spectral spreading owing to clipping. In 2001, Armstrong proposed a frequency domain filtering of the clipped signals in [25], to solve the issue of in-band distortions and out-of-band radiations. The proposed filter consists of two DFT (FFT) operations. Signals are transformed back into the DFT domain by the use of forward DFT. Through this process, the out-of-band components are nullified and the frequency components of the clipped signals that were in-band are allowed to pass. Signals are then, converted back into the time domain by IDFT. (IFFT) While this filter greatly attenuates the out-of-band components [25], it has a very little effect on in-band frequency domain components. The clipping and filtering operations are usually performed iteratively to lower the peak values of HPA into the linear region due to the occurrence of a peak regrowth. As a result, there's a growth in computational complexity in this system. The computational complexity can be reduced by optimizing C&F to obtain the marked value sooner involving minimum iterations [28].

Although clipping's simplicity to implement at the transmitter is its biggest advantage; however, iterative clipping and filtering add additional complexity.

2.2.2. Selected Mapping

Bäuml, Fischer, and Huber proposed Selected Mapping (SLM) for the first time in [29]. The conversion of original OFDM frame into independent sub blocks $\mathbf{\mathring{U}}$, having the same information is the basic idea behind SLM. These frames are obtained by multiplying the original data vector with $\mathbf{\mathring{U}}$ phasor vectors. After converting their domain to the time by applying IFFT, transmission is done by the frame with the smallest PAPR, is transmitted.

We assume that **A** is the original data vector and **P** shows the generated independent phasor vectors. The phasor vectors are usually produced with a phase difference of ($\pi/2$) [29].

Taking the IDFT, the signal in time domain is gained. After the IDFT, the selection of frame with the smallest PAPR is done and that frame is then used for data transmission.

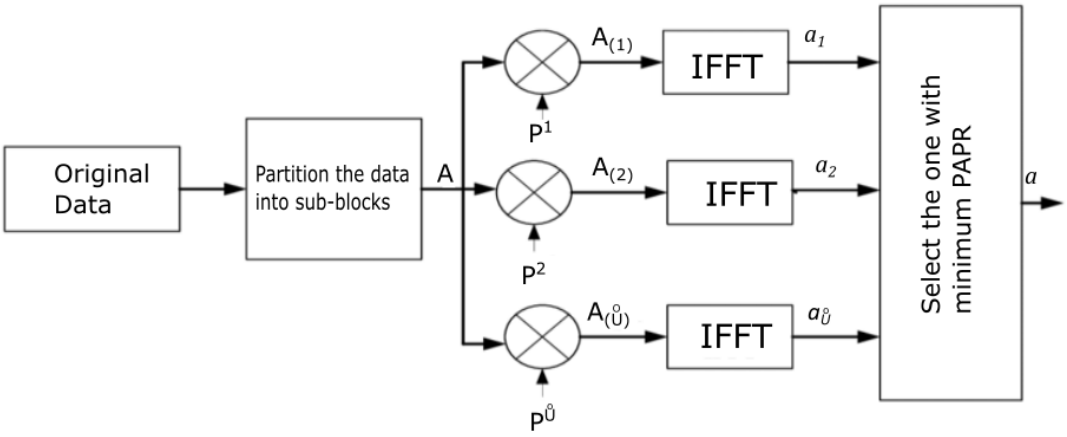

Figure 2.1 Block diagram of SLM

On the receive side, the original OFDM frame can be estimated by sending used phase vector information. At the receiver side, the original OFDM data frame is recovered by applying the DFT (FFT) and using the side information about the phase vector applied at the transmitter.

SLM is a simple method to reduce the PAPR of the system but its computational complexity increases with an increase in Ů, the number of translated OFDM frames.

2.2.3. Partial Transmit Sequences

PTS was proposed by M*ü*ller and Huber in [30]. PTS, first, partitions the input data vector containing N symbols into J sub-blocks and then each sub-block is multiplied by a phase factor. The value of the phase factor is adjusted such that it gives reduced PAPR when the signal is combined as compared to the PAPR before using the technique. PAPR reduction, in this case, is dependent on the number of sub-blocks and phase vectors. Fig 2.2 [31] shows the block diagram of the PTS technique.

PTS performs a little better than SLM result-wise [33][34]. However, its computational complexity is high, as its optimization block searches for ideal phase vectors for all the sub-blocks, which yields a low peak signal output.

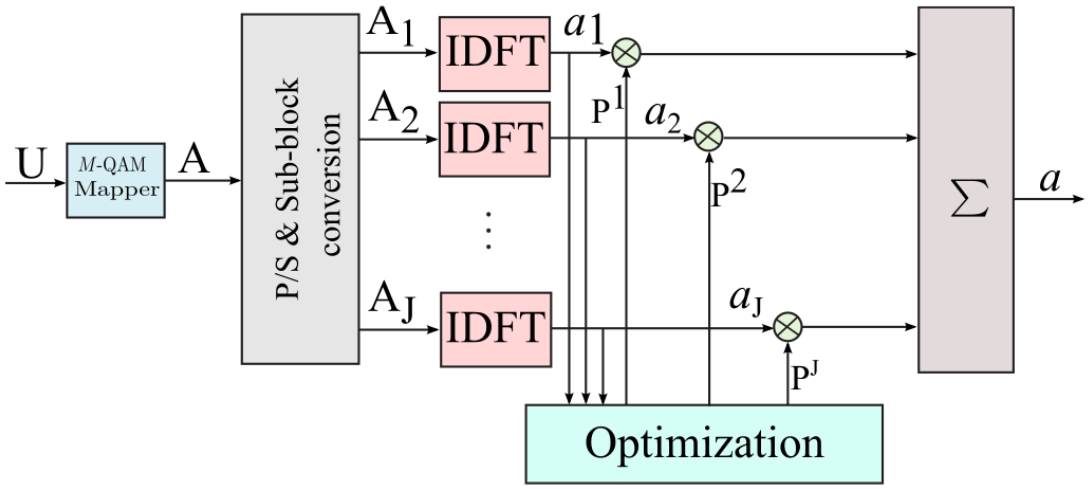

Figure 2.2 Block diagram for PTS

2.2.4. Tone Reservation

Tone Reservation was first proposed by Tellado in [33] and [34]. In the TR algorithm, a peak reduction signal is added (/subtracted) for peak reduction to the original timeline signal. A certain number of tones are reserved to generate this time-domain peak reduction signal. Therefore, the total number of tones are divided into two disjoint sets, a set of tones used for data transmission $\bar{\mathbf{A}}$ and another set of tones, called reserved tones $\mathbf{A_{res}}$, used for generating the peak reduction signal.

We suppose that $\mathbf{A} = \bar{\mathbf{A}} + \mathbf{A_{res}}$, where $\bar{A}$are the tones reserved for data transmission and $\mathbf{A_{res}}$ are the reserved tones for the purpose of PAPR reduction. $\mathbf{A_{res}}$ is used to create a corrective function (it produces a high impulse at one point) $\boldsymbol{a}_{\mathbf{res}}$, which will then be added iteratively to the initial signal $\boldsymbol{a}$ to decrease PAPR in time domain.

$$a = \text{IDFT}\{\text{A}\} = \text{IDFT}\ \{\bar{A} + \text{A}_{\text{res}}\} \tag{2.16}$$

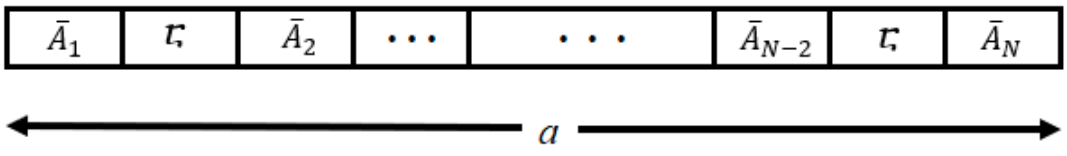

Figure 2.3 An OFDM frame depicting the reserved tones

The steps for TR algorithm are as follows:

1. Set the information vector to be represented by A, with the reserved tones set to zero.
2. Perform IFFT, i.e., $\boldsymbol{a}$ = **IFFT(A)**; to change $\boldsymbol{a}$ into time domain.
3. Determine the peak value $\boldsymbol{a_v^{(i)}}$, also the position **v** for which $|\boldsymbol{a_v^{(i)}}|$ = $\mathbf{max}_k$ $|\boldsymbol{a_k^{(i)}}|$.
4. If $|\boldsymbol{a_v^{(i)}}| < \boldsymbol{\tau}$ or if $\boldsymbol{i} > \boldsymbol{i}_{\mathbf{max}}$, the algorithm should stop and transmit $\boldsymbol{a}^{(\mathbf{i})}$.
5. else,

$$a^{(i+1)} = a^{(i)} - ɗ(a_v^{(i)} - e^{j\,arg\{a_v^{(i)}\}}.\tau)(a_{\text{res}}(\text{N} - \text{m}) \text{ modulo N}) \qquad (2.17)$$

6. $i = i + 1$, go to step 4, where

where $i := i + 1 \rightarrow i \leq 3$and

- Step size is ɗ
- i^{th} iteration by i
- peak position by v
- phase of complex vector a_k by arg a_k
- threshold value by τ
- time-shifted version of a_{res} by $a_{\text{res}}(\text{N} - \text{m})$
- threshold overshoot is defined by $(a_v^{(i)} - e^{j\,arg\{a_v^{(i)}\}}.\tau)$

2.3. PAPR Reduction Techniques in MIMO Systems

The algorithms defined for the PAPR reduction in SISO can be extended for MIMO-OFDM but it is not the case in multiuser MIMO-OFDM. The complexity of the above-mentioned PAPR reducing algorithms also increases linearly with the M_t and the type of MIMO deployment scenario being considered. As an example, these algorithms can be directly extended to each transmit antenna in a single-user p-to-p MIMO-OFDM system as signal processing at both the transmit as well as the receive end is possible. It is guaranteed that the algorithm's complexity will increase by M_t times as compared to the SISO systems, where the total number of transmit antennas

is M_t. Likewise, in the case of multi-user multiple access channel (MAC) scenario in which each user has a single transmit antenna, the algorithms mentioned in Section 2.2 are simply SISO systems scenarios that have been extended. Here, a short summary of some of the PAPR reduction techniques used in MIMO systems are presented.

2.3.1. Selected Mapping / Partial Transmit Sequences

The main working principle of SLM and PTS (i.e., to produce multi replicas of the same symbol at each transmit antenna) for MIMO systems is the same as that of SISO systems, therefore, can be extended in a similar way.

To combat the severe effects of high PAPR in MIMO systems, various modified versions have been introduced for SLM and PTS in [43]–[52]. In [35], the authors used SLM for reducing the PAPR of STBC-MIMO systems with much accurate side information than in individual SLM.

In [36], the authors presented new variants of SLM for p-to-p MIMO systems. These variants were known as the ordinary SLM (o-SLM) and the simplified SLM (s-SLM), and they have same computational complexity defined as $Ů \cdot M_t$ IFFT modulators. The o-SLM is a directly extended version of the SLM in the MIMO technology but as compared to o-SLM, all transmit antennas in the s-SLM use the same phasor vectors. Similarly, the authors also proposed the new variants for PTS i.e., o-PTS and s-PTS.

In [39], the d-SLM was presented for P-to-P MIMO systems. In d-SLM, antenna with worst PAPR is the main focus and it has a better performance than the o-SLM and s-SLM. The same approach was use for PTS, i.e., d-PTS. In [41], a new SLM variant SLS was proposed by Siegel.

2.3.2. Tone Reservation

Similarly, the TR algorithm is also extended for MIMO-OFDM systems. In [45], the authors generated a corrective signal on the tones not used for data transmission. The second order cone programming also known as SOCP performs optimization on the corrective signal, but the major drawback of this proposed

technique is the increase in the mean power of transmit signal. Even with using a mean power constraint the results are not very promising.

2.3.3. Least Square (LS)

In [46], Wakeel and Henkel used the weakest eigenchannels for the approximation of the peaks excursions beyond a fixed threshold value by using least square method. This approximated signal is then subtracted in time domain from the original signal for PAPR reduction. The proposed method is an iterative method as the estimation of peaks exceeding the set target value is not possible in one iteration using this method. This method gives high gains with a insignificant increase in average power and system's capacity loss.

2.4. PAPR Reduction Techniques in Massive MIMO

Massive MIMO also known as large scale MIMO has become the focus of all researchers as a possible technology for 5G. With larger numbers of antennas involved in transmitting of data, PAPR in Massive MIMO system is tremendous. Many previously mentioned techniques have been modified and new PAPR reduction methods have been proposed with varying level of success. As there is always a trade-off between PAPR and other performance parameters, a lone technique cannot be referred as the go-to method for PAPR reduction.

2.4.1. BD-SLM

In [47], Shusaku Umeda et. al. proposed a technique named as **BD-SLM**, as it uses block diagonal (BD) precoder for the PAPR reduction in massive MIMO-OFDM. This technique is a modified form of SLM.

The proposed **BD-SLM** method enables Eigenmode transmission SLM (EM-SLM) to be applicable to a multi-user MIMO-OFDM system. A phase shift of all the modulated signals is performed by **BD-SLM,** before applying the linear pre-code. A selection of a suitable phase sequence is performed by the proposed method, that minimizes the peaks of transmit signals at all antennas.

From simulation results, it is proved that **BD-SLM** performs better than the normal BD transmitter. **BD-SLM** reduces PAPR by more than 3dB at 10^{-3} as compared to normal BD transmitter and this reduction in PAPR also reduces the average packet error rate (PER).

2.4.2. Simplified Iterative Discrete Estimations (SIDE)

Ting Liu et. al. proposed a technique named as **Simplified Iterative Discrete Estimation (SIDE)** in [48]. **SIDE** is a precoder that takes advantage of the many key characteristics of massive MIMO-OFDM-ADMA system model and effectively reduces its PAPR with comparatively lesser computation complexity. To reduce the computational complexity, the precoding factor **β** from **MMSE** is simplified for **SIDE** algorithm, defined as

$$\beta = \sqrt{\frac{\mathrm{tr}\left(\left(\dot{\mathbf{H}}\dot{\mathbf{H}}^{\mathrm{H}}\right)^{-1}\right)}{MP_t}} \tag{2.18}$$

The results of SIDE simulations show that it can produce almost ideal PAPR reduction with barely any symbol error ratio (**SER**) performance deterioration. The authors compared SIDE with MF precoder for reference in their work.

2.4.3. ADMM approach

In [49], Hengyao Bao et al proposed a perturbation signal assisted approach. This technique works by adding carefully formulated artificial perturbation signals to the preprocessed signals for the purpose of PAPR reduction of the transmit signals. They put constraints on these signals that do not allow any MUI or out-of-band radiations as the formulated signals lie between the null space of its two adjacent signals. While considering the reduction in PAPR as a convex problem, the authors used the splitting of variables and the **Alternating Direction Method of Multipliers (ADMM)** method for the development of their algorithm.

The simulation results show that the proposed algorithm has a very fast convergence rate as it converges in the first ten iterations and, has a high rate of PAPR reduction.

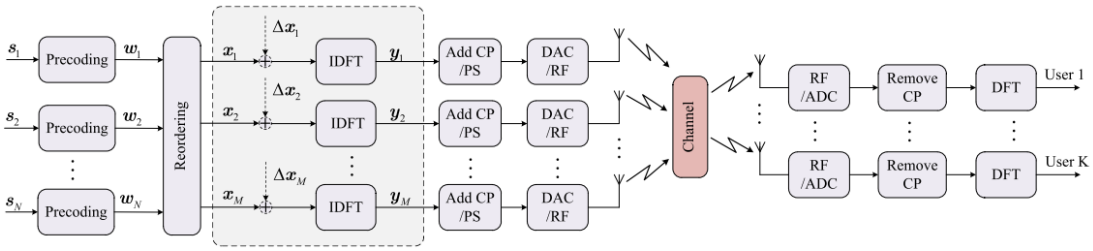

Figure 2.4 system model of the massive multi-user MIMO-OFDM downlink scenario

2.4.4. Clipping & Filtering

In [50], Tomoya Kageyama et al proposed a modified version of the clipping and filtering method for the objective of reducing PAPR in massive MIMO-OFDM systems. The authors proposed a filter to limit the out-of-band radiation by clipping and using filtering to reduce the possibility of regrowth of peak amplitude. The effect of using extra antennas was also discussed for compensating the in-band distortion caused by clipping and filtering in massive MIMO.

The results show us that in terms of PAPR, ACLR, and SDR, the modified algorithm gives an efficient reduction in the peak amplitude of our concerned category.

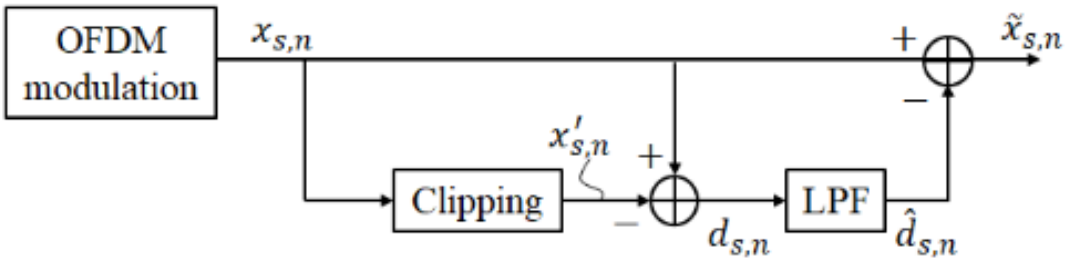

Figure 2.5 The modified C&F block

2.4.5. Adaptive Peak Cancellation

In [51], Tomoya Kageyama et al proposed an analytic method to estimate the realizable BER with the adaptive peak cancellation in downlink massive MIMO-OFDM systems using different numbers of antennas at the transmitter side and the

users. The massive MIMO-OFDM system with peak cancellation is pre-coded with maximum ratio combining (MRC).

According to this analytic method, bit error rate (BER) is calculated assuming that the in-band distortion is approximated that was generated because of peak cancellation. The theoretically calculated BER shows a similar result as in the simulated results. Moreover, the authors also discussed the effect of increase in number of transmit antennas on parameters like BER and reduction in PAPR.

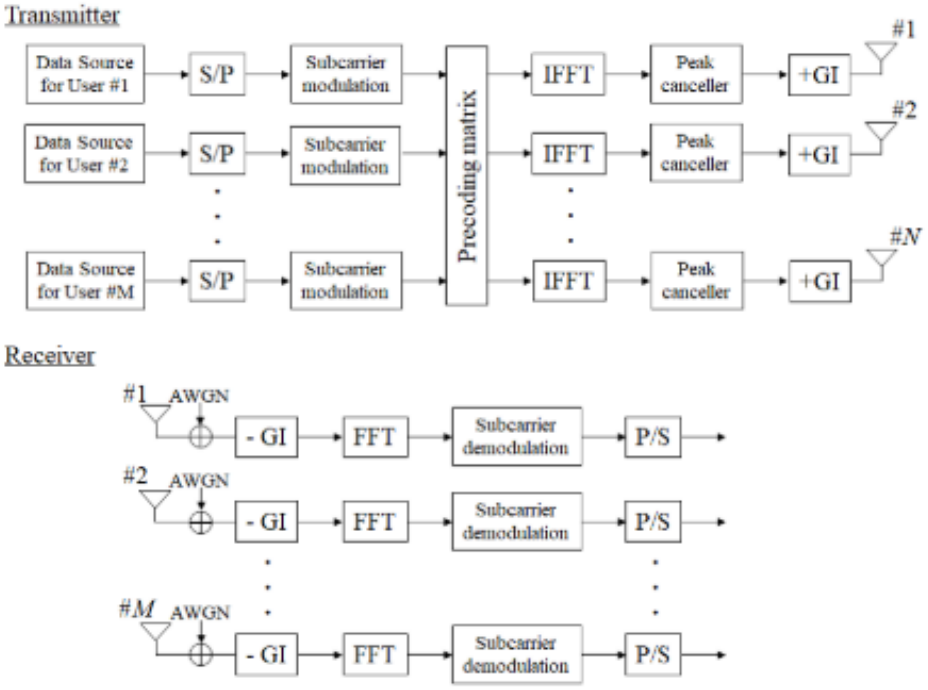

Figure 2.6 block diagram for massive MIMO system depicting peak cancellation

2.4.6. UBR

In [52], Andrey Ivanov et al proposed unused beam reservation (UBR) algorithm PAPR reduction in the downlink channel of largescale MU-MIMO system.

The MMSE-based UBR algorithm works by estimating the complex amplitudes of the unused beams on every sub-carrier. The unused beams are determined by removing the pre-processing matrices of active users from the overall set of precoding matrices. From simulated results, it is obvious that the proposed method UBR gives good results. But it also verifies that the combined form of

selective TR (STR) and UBR algorithms produces better results than both the STR and UBR in Massive multi-user MIMO.

2.4.7. SDR based Approach

In [53], Miao Yao et al proposed an SDR-based approach to reduce PAPR in mMIMO-OFDM systems.

As in the largescale MIMO, we have a large number of BS antennas than that of users'; the proposed technique takes advantage of extra antennas at the transmitter side to apply a constraint on every antenna for a PAPR constrained signal. To reduce the rank of the SDR solution, we apply a method based upon the randomization process. The authors also designed a PAPR-aware precoding solution for massive MIMO-OFDM intercell coordination. The numerical results show that PAPR is reduced for different scenarios involving an individual cell, users at cell-edge, and multi-cells (catering to center-cell).

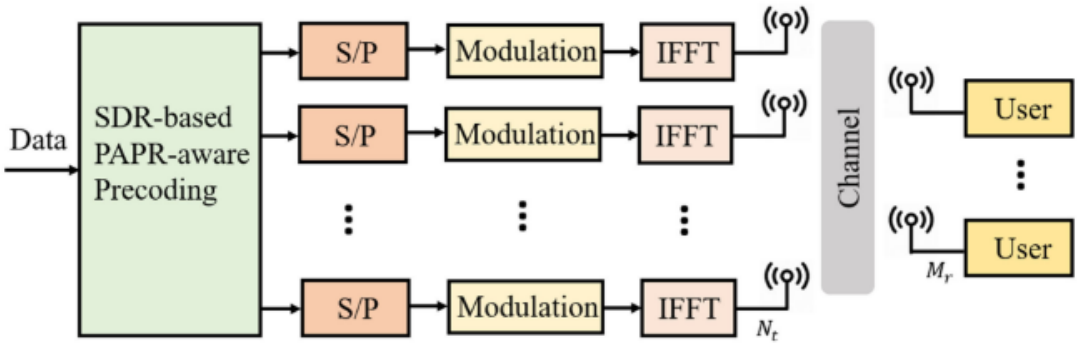

Figure 2.7 block diagram of the proposed method

2.4.8. Enhanced Peak Cancellation

In [54], Tomoya Kageyama et al proposed an enhanced peak cancellation scheme by using [51] with simplified in-band distortion compensation for massive MIMO-OFDM.

The compensation of an in-band distortion caused by peak cancellation is done by transmitting a compensation signal on extra transmit antennas. Moreover, by

using this method, the reduction of a high peak is possible without any BER performance degradation. This method can also be used for non-linear pre-coded massive MIMO-OFDM systems. In non-linear systems, the cancellation signal is superimposed on the compensation signal which results in a signal that is simply demodulated on the receiver side; so, there is no need to perform non-linear processing to remove the perturbation vector at receiver.

The results calculated show the performance of the scheme by using parameters CCDF, SDNR and BER.

2.4.9. TR Algorithm

In [55], Christian A. Schmidt et al proposed an algorithm based on combining TR algorithm with the digital beam steering for a massive MIMO-OFDM system. This scheme works by keeping each antenna's individual weight constant and to get a highly accurate control on the routing of beams. As this allows the power amplifiers to work at the same input power back-off, the energy efficiency gained by using this PAPR reduction method is high.

The computational intricacy of the proposed technique is much lower than to frequency domain beamforming and the scheme improves the PAPR.

2.4.10. Machine Learning Approach

In [56], Aleksei Kalinov et al proposed to use machine learning (ML) approach for PAPR reduction in the downlink channel large-scale MIMO-OFDM. After spreading the noise across the frequency and spatial domains according to the maximum allowed value of error vector magnitude (EVM), a significant PAPR reduction is achieved. This approach involves the manual tuning of hyper-parameters for each scenario; thus, it is quite time-consuming. They proposed to use ML optimized linear ridge estimation for the calculation of hyper-parameters instead of using brute force.

The authors observed that the identification and saving of the optimal parameters for different scenarios is not possible practically in the applications of the STR [57] and UBR [52] algorithms. Kalinov et al proposed to use ML-based

reconstruction of these parameters. In STR and UBR algorithms, the requirement was to sort the highest peaks for different parameters (resource block (RB) numbers); which is time-consuming and expensive. The authors proposed a threshold approach to get our peaks instead of using brute force and convert them from a discrete optimization problem to a continuous one. Then for the construction of a parametric model from the set of hyperparameter values, we use the classic ML algorithm.

The simulation results show that the proposed method produces efficient and fast results by the factor of hundreds of times. The implementation complexity is negligible and the time taken for calculations is also smaller than the brute force one. The proposed ML approximation speeds up the optimization by a factor of hundreds without reducing the quality of performance.

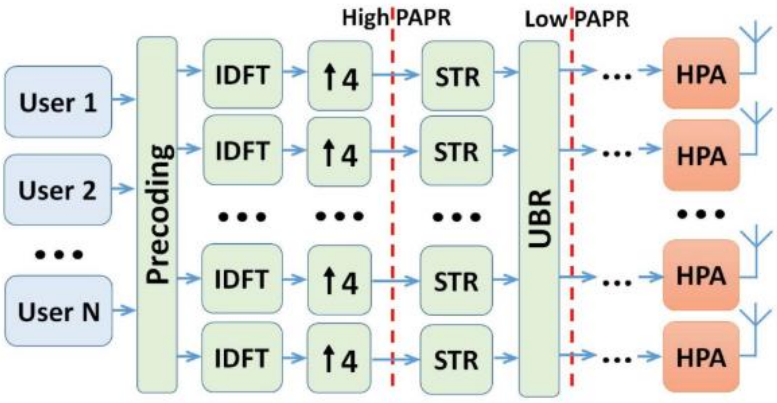

Figure 2.8 Functional workflow for PAPR reduction

Chapter 3:

Novel Adaptive Beam Reservation Algorithm for PAPR Reduction in P-to-P Massive MIMO-OFDM System

In this chapter, we will discuss our proposed Beam Reservation (BR) algorithm to reduce the PAPR in a P-to-P massive MIMO-OFDM system. In a P-to-P MIMO-OFDM scenario, it is possible to do co-processing of the signal at both the transmitter and receiver ends using pre-processing matrix at the transmitter side and post-processing matrix at the receiver side. In the case of P-to-P, the gain of the last Eigen channel(s) is too low and is not used for data transmission. We will use it to provide redundancy to reduce PAPR for a MIMO-OFDM system. In the proposed BR algorithm, we discuss the design of an ideal spiky function using unused Eigen channels. Like the TR algorithm, the proposed spikey function is then added to the transmit signal iteratively to reduce the PAPR.

3.1. Adaptive BR Algorithm for PAPR Reduction in MIMO-OFDM Systems

One of the most straightforward and least complex technique that is used for PAPR reduction in MIMO-OFDM systems is known as Tone Reservation. As we recall from the previous chapter, the algorithm tends to reserve a specific number of tones out of all the available tones. These reserved tones are then used to produce a spiky function, that is added to transmit signal iteratively to reduce the high amplitude of the transmit signal that extends across asset threshold value τ. This algorithm was at first proposed for the SISO-OFDM systems and may also be applied to MIMO-OFDM without any extreme change in it. In [45], for a P-to-P

MIMO-OFDM with Alamouti-coding, the researchers proposed to reserve tones to reduce PAPR.

Herein, a new method for generating the spiky function is introduced in our proposed BR algorithm. In traditional TR, the reserved tones are used to generate an optimum spiky function that spans all spatial dimensions. The difference in this algorithm to that of the conventional approach is that the weakest Eigen channels, not suitable for data transmission, are used to generate an ideal spiky function.

3.1.1. Key idea

With the assumption of a p-to-p MIMO-OFDM system, we take the transmitter-sided pre-processing and receiver-side post-processing with perfect CSI on both sides. Consider, the number of transmitting antennas ($\mathbf{M_t}$) is equivalent to that of the number of the receiving antennas i.e., $\boldsymbol{M_t = M_r = M}$; we can define the channel gain matrix as,

$$\mathbf{H}(n)=\begin{pmatrix} h_{1,1} & h_{1,2} & \cdots & h_{1,M} \\ h_{2,1} & h_{2,2} & \cdots & h_{2,M} \\ \vdots & \vdots & \ddots & \vdots \\ h_{M,1} & h_{M,2} & \ldots & h_{M,M} \end{pmatrix} \tag{3.1}$$

By applying single value decomposition (**SVD**) on $\mathbf{H}(n)$, we get

$$\mathbf{H}(n) = \mathbf{C}(n) \,.\, \Delta(n) \,.\, \mathbf{E^H}(n) \tag{3.2}$$

Here, $\mathbf{C}(n)$ and $\mathbf{E}(n)$ represents the matrices of post-processing and pre-processing function, correspondingly ($\mathbf{C^H . C = E^H . E = I}$) and $\boldsymbol{\Delta(n)}$ represents the diagonal matrix which contains the singular values of the channel gain matrix $\mathbf{H}(n)$, i.e.,

$$\Delta(n) = \begin{bmatrix} \delta_{1,1}(n) & 0 & \ldots & 0 \\ 0 & \delta_{2,2}(n) & \ldots & 0 \\ \vdots & \vdots & \ddots & \vdots \\ 0 & 0 & \ldots & \delta_{M,M}(n) \end{bmatrix} \tag{3.3}$$

By using the **SVD** algorithm, we get the diagonal matrix in which the singular values of matrix **H** are arranged in descending order (i.e., $\boldsymbol{\delta_{1,1} \geq \delta_{2,2} \geq \ldots \geq \delta_{M,M}}$) and the last value $\boldsymbol{\delta_{M,M}}$ is being the smallest.

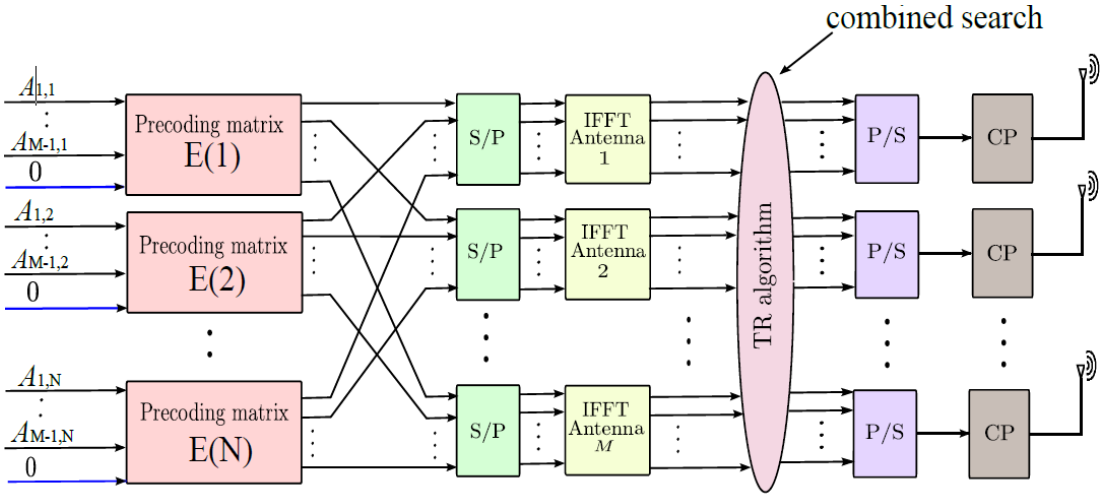

Figure 3.1 Transmitter system model with BR algorithm

The last gain is so small that data transmission is not profitable. omitting to use them would provide PAPR redundancy without much data rate costs. As a result, we will set aside the Eigen channels having the smallest gain to generate a corrective function, that is applied for PAPR reduction.

3.1.2. System Model

We assume a p-to-p MIMO-OFDM with transmitter antennas $\mathbf{M_t}$ and receiver antennas M_r. Suppose $\mathbf{A}(n)$ is the input data then it is pre-processed with $\mathbf{E}(n)$ at the transmitter side. After pre-processing, the outcome is then passed through an S/P converter. Afterward, we perform the IFFT on the parallel data signal to convert it into the time domain. The converted frame is then appended with a CP to minimize the channel impairments, i.e., ISI. The obtained CP padded signal is then transmitted.

To estimate the transmitted signal at the receive side, we perform reverse operations. The signal that is to be transmitted $\mathbf{A}(n)$ is pre-processed by $\mathbf{E}(n)$, while the received signal is post-processed by $\mathbf{C^H}(n)$ to get the output vector $\mathbf{B}(n)$ as revealed in Fig 3.2.

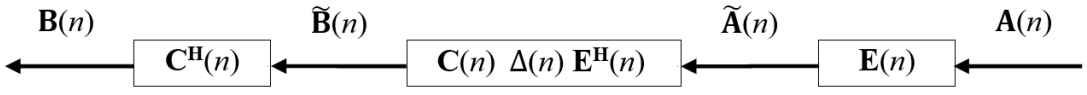

Figure 3.2 Using SVD for the diagonalization of MIMO Channel

$$\tilde{\mathbf{B}}(n) = \mathbf{H}(n).\tilde{\mathbf{A}}(n) + \mathbf{W}(n)\ , \tag{3.4}$$

where $\mathbf{W}(n)$ represents the AWGN of the channel. After multiplying with $\mathbf{C^H}(n)$, we get

$$\mathbf{B}(n) = \mathbf{C^H}(n).\ \widetilde{\mathbf{B}}(n) = \mathbf{C^H}(n)\ .\ \mathbf{H}(n)\ .\ \widetilde{\mathbf{A}}(n) + \widetilde{\mathbf{W}}(n) \tag{3.5}$$

$\widetilde{\mathbf{W}}(n) = \mathbf{C^H}(n)\ .\ \mathbf{W}(n)$ as a result of $\mathbf{C^H}(n)$ been a unitary matrix. Similarly $\widetilde{\mathbf{A}}(n) = \mathbf{E}(n)\ .\ \mathbf{A}(n)$. By applying SVD on $\mathbf{H}(n)$, we get $\mathbf{H}(n) = \mathbf{C}(n)\ .\ \mathbf{\Delta}(n)\ .\ \mathbf{E^H}(n)$ and by ignoring $\mathbf{W}(n)$, we get

$$\mathbf{B}(n) = \mathbf{C}\ (n)^H\ .\ \mathbf{C}\ (n)\ .\ \Delta\ (n)\ .\ \mathbf{E^H}\ (n)\ .\ \mathbf{E}\ (n)\ .\ \mathbf{A}\ (n) \tag{3.6}$$

Using the relations $\mathbf{C^H}(n)\ .\ \mathbf{C}(n) = \mathbf{E^H}(n)\ .\ \mathbf{E}(n) = \mathbf{I}(n)$, Eq 3.6 becomes

$$\mathbf{B}(n) = \mathbf{\Delta}\ (n)\ .\ \ \mathbf{A}\ (n) \tag{3.7}$$

With the assumption $M_t = M_r = M$, Eq 3.7 in matrix form is

$$\mathbf{B}(\mathrm{n}) = \Delta(n).\mathbf{A}(n) = \begin{pmatrix} \delta_{1,1}(n) & 0 & 0 & 0 \\ 0 & \delta_{2,2}(n) & 0 & 0 \\ 0 & 0 & \ddots & 0 \\ 0 & 0 & 0 & \delta_{M,M}(n) \end{pmatrix} \begin{pmatrix} A_{1,n} \\ A_{2,n} \\ \vdots \\ A_{M,n} \end{pmatrix} \tag{3.8}$$

According to our algorithm, $\boldsymbol{\delta_{M,M}(n)}$ is the only dimension reserved for PAPR reduction, and all the others are being used for the transmission of data. $\mathbf{D(}\boldsymbol{n}\mathbf{)}$ is assumed to be the vector used for data transmission, i.e.,

$$\mathbf{D}(n) = (A_{1,n} \quad A_{2,n} \quad \ldots \quad A_{M-1,n} \quad 0)^T \tag{3.9}$$

Whereas, $\mathbf{G}(n)$ defines the reserved dimension for PAPR reduction, defined as

$$\mathbf{G}(n) = (0 \quad 0 \quad \ldots \quad 0 \quad G_n)^T \tag{3.10}$$

In conventional **TR** algorithm, some of the tones are reserved on which the generation of spiky function is done. In our proposed algorithm, we will use $\mathbf{G}(n)$ to generate a spiky function. The $\mathbf{D}(n)$ and the $\mathbf{G}(n)$ are then pre-coded as

$$\widetilde{\mathbf{D}}_n = \mathbf{E}(n).\mathbf{D}(n) = \mathbf{E}(n).(A_{1,n} \quad A_{2,n} \quad \ldots \quad A_{M-1,n} \quad 0)^T \tag{3.9}$$

$$\widetilde{\mathbf{G}}_{\mathrm{n}} = \mathbf{E}(n).\mathbf{G}(n) = \mathbf{E}(n)\ .(0 \quad 0 \quad \ldots \quad 0 \quad G_n)^T \tag{3.10}$$

We perform IFFT to convert them into time-domain ($\tilde{\mathbf{d}}^T = \mathbf{F^{-1}}\ \tilde{\mathbf{D}}^T$ and $\tilde{\mathbf{g}}^T = \mathbf{F^{-1}}\ \tilde{\mathbf{G}}^T$); where $\mathbf{F^{-1}}$ defines IFFT matrix. $\tilde{\mathbf{g}}^{\mathbf{T}}$ is the spikey function that is added iteratively to the time domain signal $\tilde{\mathbf{d}}^T$ for PAPR reduction. The overall equation becomes

$$\tilde{\mathbf{a}} = \tilde{\mathbf{d}} + \tilde{\mathbf{g}} = \mathbf{F^{-1}}\ \mathbf{E}\ \mathbf{A} = \mathbf{F^{-1}}\ \mathbf{E}\ (\mathbf{D} + \mathbf{G}) \tag{3.11}$$

Now, we need to design an ideal spiky function by utilizing the last reserved Eigen channels **G**, so that it reduces peak excursions that exceed a threshold τ.

3.1.3. A Spiky Function

We propose a new design for an ideal spiky function $\mathbf{G_n}$ that can be calculated as,

$$G_n = E^*_{\mu,M}(n) \tag{3.12}$$

where * is the complex conjugate. When a dimension and its conjugate are multiplied, they give real values at that particular dimension; so, on that dimension (at time zero), we observe a high peak at that dimension. However, it becomes an advantage as this spikey function never allows the peaks on other dimensions to exceed the peak on our intended dimension. After some simplifications and an IFFT, we can obtain the time domain signal as

$$\tilde{\mathbf{g}}^{\boldsymbol{\mu}} = \mathbf{F}^{-\mathbf{1}}.\mathbf{E} = \begin{bmatrix} 0 & \dots & 0 \\ \vdots & \dots & \vdots \\ 0 & \dots & 0 \\ G_1^{\mu} & \dots & G_N^{\mu} \end{bmatrix} \tag{3.13}$$

For PAPR reduction, we add the corrective function $\tilde{\mathbf{g}}$ iteratively to $\tilde{\mathbf{d}}$.

3.2. Beam Reservation algorithm

Our proposed BR algorithm can be summarized as

1- Set **D** as the data matrix in the frequency domain with the reserved dimension for the spiky function set to zero. Similarly, we also set **G** to

be the spiky function matrix in the frequency domain with the dimension used for data transmission set to zero.

2- Pre-process the data matrix **D** and spiky function matrix **G** by multiplying with the pre-processing matrix **E**, i.e., $\widetilde{\mathbf{D}} = \mathbf{E} \cdot \mathbf{D}$ and $\widetilde{\mathbf{G}} = \mathbf{E} \cdot \mathbf{G}$.

3- Convert the frequency domain matrices $\widetilde{\mathbf{D}}$ and $\widetilde{\mathbf{G}}$ to time-domain, i.e., $\tilde{\mathbf{d}} = \mathbf{F^{-1}}\widetilde{\mathbf{D}}$ & $\tilde{\mathbf{g}} = \mathbf{F^{-1}}\ \widetilde{\mathbf{G}}$. The Initial value of the iteration counter $\boldsymbol{i}$ is set as zero.

4- Find the value $d_{m,\mu}^{i}$ and location *m*, for the signal $\tilde{\mathbf{s}}$ in time-domain, where $\left|\boldsymbol{d}_{\boldsymbol{m},\boldsymbol{\mu}}^{\boldsymbol{i}}\right| = \mathbf{max}_{\boldsymbol{k}}\left|\boldsymbol{d}_{\boldsymbol{k}}^{\boldsymbol{i}}\right|$.

5- If $\boldsymbol{d}_{\boldsymbol{m},\boldsymbol{\mu}}^{\boldsymbol{i}} < \boldsymbol{\tau}\ \boldsymbol{or}\ \boldsymbol{i} > \boldsymbol{i}_{\boldsymbol{max}}$ then stop the process and transmit $\tilde{\mathbf{d}}^{\mathbf{i}}$, or else

6- Time-domain vector is updated as

$$\tilde{\mathbf{d}}^{\mathbf{i+1}} = \tilde{\mathbf{d}}^{\mathbf{i}} - \text{ɗ}.(\mathbf{d}_{\boldsymbol{\mu},\mathbf{m}}^{\mathbf{i}} - e^{-j\ arg(d_{\mu,m}^{i})\tau}).(\tilde{\mathbf{g}}^{\boldsymbol{\mu}} \rightarrow m) \qquad (3.14)$$

And if $i = i+1$, we return to to step 4.

Step 6 shows the working of our BR algorithm at an antenna μ at the transmitter for a peak, where $\mu = 1, 2, \ldots, M_t$ and position *m*, with μ^{th} spiky function $\tilde{\mathbf{r}}^{\boldsymbol{\mu}}$. The *i* shows the iteration numbering, $\tilde{\mathbf{d}}$ defines the $M_t \times N$ data in the time-domain and N describes the IFFT length.

3.3. Simulations

As it is possible to do joint signal processing in a P-to-P MIMO-OFDM system, the average power gets distributed over all sub-carriers because of the pre-processing done at the transmitter side. However, as we are including a signal in the time-domain carrying the spiky function $\tilde{\mathbf{g}}$ to the original data $\tilde{\mathbf{d}}$ for PAPR reduction; each iteration pass slightly adds to the average power. After using the TR algorithm, we can define the PAPR as

$$PAPR = \frac{\max\limits_{\forall_\mu, \forall_k} \left|\mathrm{d}_{\mu,k} + \mathrm{g}_{\mu,k}\right|^2}{\sigma^2} \qquad (3.15)$$

Where, $\boldsymbol{\sigma^2 = E_{\forall_\mu,\forall_k}\left\{\left|a_{\mu,k}\right|^2\right\}}$ is the average power without any PAPR reduction and *k* is the sampling index.

With $\boldsymbol{l_h}$ **=15** as the channel length, we select the channel matrix as in [41]. Exact CSIs are considered at the transmitter. For simulation, we chose **10×10** and **50×50 MIMO-OFDM** systems with sub-carriers ***N*=128** and modulation of **16-QAM**. Complementary cumulative distribution function (CCDF) is used to check and compare the performance of the system. CCDF determines the probability of current PAPR exceeding a predefined threshold τ, i.e., P_r {PAPR > τ}, it can be determined as,

$$P_r\{\text{PAPR} > \tau\} = 1-(1-e^{-\tau})^{\text{N M}} \tag{3.16}$$

The peak values, across all spatial dimensions that cross a predetermined value τ, are searched by the algorithm, for the reduction of PAPR (of the signal transmitted). Then following step 6 of the algorithm, the spiky function is cyclically shifted to the highest peak position and is subtract from **d**.

The algorithm only processes one peak at a time, the other peaks on the remaining dimension may grow, thus there is a high probability o that the algorithm is performed iteratively. There are two ways to search for the highest peak

1- The first method is the combined search method that searches a high peak on all spatial dimensions.
2- The second method is the individual search that is carried out on each dimension by distributing the determined iterations in equal numbers amongst all antennas, i.e., $\boldsymbol{i_{max}}$ **/ M**. In this way, the search is carried out for a given number of iterations on one antenna at a time. It is done by ignoring the peak regrowths on the other antennas. The spiky function is then applied at that antenna for the reduction of PAPR of that corresponding antenna.

Moreover, we perform

1. PAPR reduction in massive MIMO-OFDM
2. PAPR reduction under mean power constraints
3. Capacity/ Rate loss due to the proposed BR solution
4. Performance comparison with conventional TR algorithm

3.3.1. PAPR reduction using BR algorithm

To analyse the PAPR reduction capability of our proposed BR algorithm, we consider a 10×10 and 50×50 MIMO-OFDM systems. The number of subcarriers M=128 then we consider a 16-QAM constellation.

3.3.1.1. Simulation results for combined search

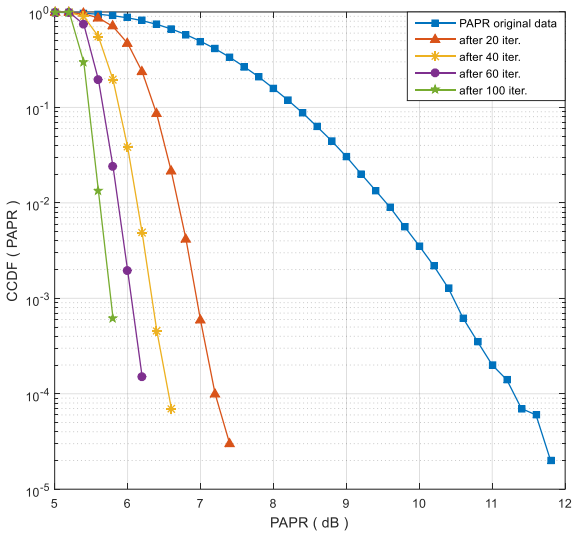

Figure 3.3 PAPR curves for a 10×10 MIMO-OFDM for the proposed BR algorithm, with target value = 5.5 dB; with a combined search algorithm

Fig 3.3 shows the simulation results of the combined search approach. For a 10×10 MIMO-OFDM system with a target PAPR of 5.5 dB. It is deduced from the results, that with the increasing iteration number the gain is increasing. With as few as 20 iterations, we obtain a gain of 4.4 dB at 10^{-5}. Moreover, the high number of iterations shows that our BR algorithm is converging to the target PAPR value.

Fig 3.4 shows the simulation results for a 50×50 MIMO-OFDM system with a target PAPR of 5.5 dB. A gain of 4dB is obtained with as few as 50 iterations and as high as 5dB with 250 iterations through a combined search.

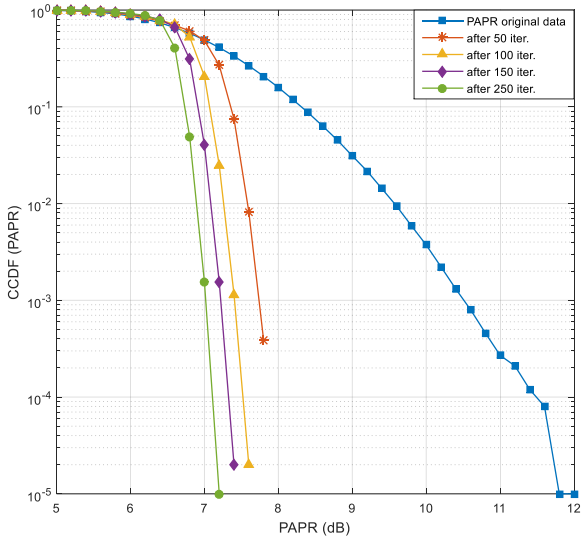

Figure 3.4 PAPR curves for a 50×50 massive MIMO-OFDM for the proposed BR algorithm, with target value = 5.5 dB; with a combined search algorithm

3.3.1.2. Simulation results for individual search

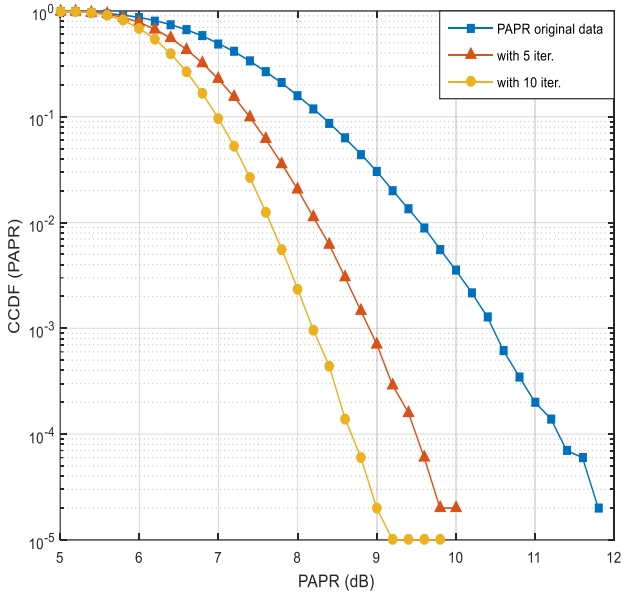

Figure 3.5 PAPR curves for a 10×10 MIMO-OFDM for the proposed BR algorithm, with target value = 5.5 dB; with a combined individual algorithm

Fig 3.5 shows the simulated results of the individual search approach for a 10×10 MIMO-OFDM system with a target PAPR value of 5.5 dB. After 10 iterations our gain is 2.6dB at 10^{-5}. It is observed that with the increasing number of iterations, the gain obtained becomes so minuscule that the CCDF of some iterations become overlapping.

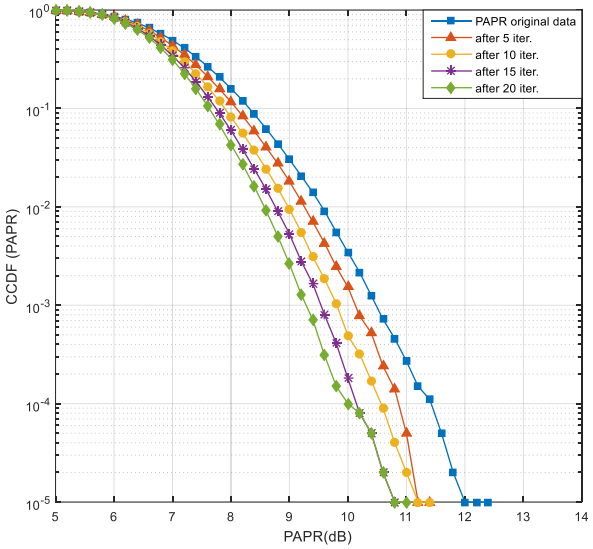

Figure 3.6 PAPR curves for a 50×50 massive MIMO-OFDM for the proposed BR algorithm, with target value = 5.5 dB; with a individual search algorithm

Fig 3.6 demonstrates the results of simulations done in individual search style for a 50×50 MIMO-OFDM system with a target PAPR value of 5.5 dB. As shown in fig 3.6 we have a gain of 1.6 dB at 10^{-5} with 20 iterations.

For P-to-P Massive MIMO-OFDM, the results show us that with the increasing number of antennas, our gain is becoming minuscule with each iteration. The results obtained by the combined search are more efficient than the ones obtained from a search done individually.

As mentioned previously, we reduce PAPR by adding a time-domain signal to the transmit signal. As a result of which, the signal's mean transmit power increases. Thus, it is important to constrain the mean power increase of the transmit signal.

3.3.2. Relative mean power increase (ΔE)

A signal $\tilde{\boldsymbol{g}}$ in the time domain, is added to the data signal $\tilde{\boldsymbol{d}}$, to reduce PAPR, to avoid the chances of clipping. However, the average transmitted power increases as a result of this. The relative mean transmit power [9] is defined as

$$\Delta E = 10\, log_{10} \frac{E\left\{\left\|\tilde{d}^i + \tilde{g}^i\right\|_2^2\right\}}{E\left\{\left\|\tilde{d}\right\|_2^2\right\}} \tag{3.17}$$

Where, $E\left\{\left|\left|\tilde{d}\right|\right|_2^2\right\}$ is the nominal average power and $E\left\{\left|\left|\tilde{d}^i + \tilde{g}^i\right|\right|_2^2\right\}$ is the average power at a specific iteration *i*.

To constrain the mean power, we need to modify step 5 of our BR algorithm. If ΔE_{Th} is the limitation on mean power then

- If $d_{m,\mu}^i < \tau \; or \; i > i_{max}$ or $\Delta E > \Delta E_{Th}$, then stop the simulations and transmit $\tilde{d}^i$.

The algorithm is now modified to check for any change in the mean power of transmit signal in addition to the maximum number of iterations i_{max} and the PAPR target value τ.

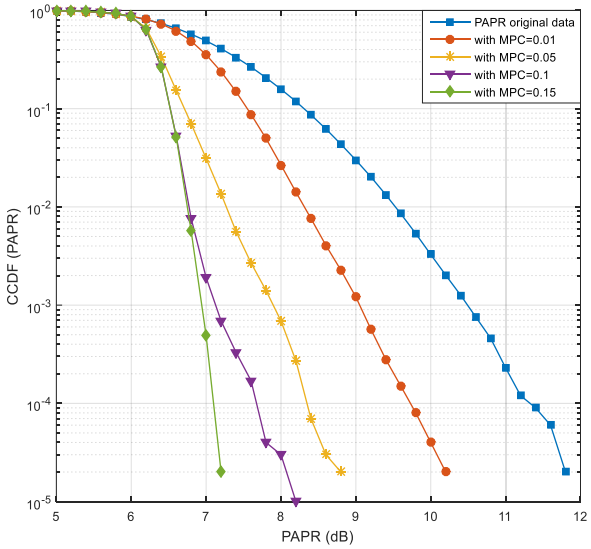

Figure 3.7 CCDF of proposed BR algorithm with different MPC values for 10×10 P-to-P MIMO-OFDM, PAPR target value = 5.5dB, using a combined search algorithm

Figure 3.7 shows the simulation results of the transmit signal $\tilde{\boldsymbol{d}}$ with the limitations of mean power constraint for a 10×10 P-to-P MIMO-OFDM using combined search. It can be observed that a gain of 4.6dB value of gain can be attained at 10^{-5} for mean power constraint of value 0.15 dB.

Figure 3.8 shows the results for a 50×50 p-to-p MIMO-OFDM system. It can be observed that around 3.6 dB gain can be obtained at 10^{-5} with a mean power increase of 0.15 dB.

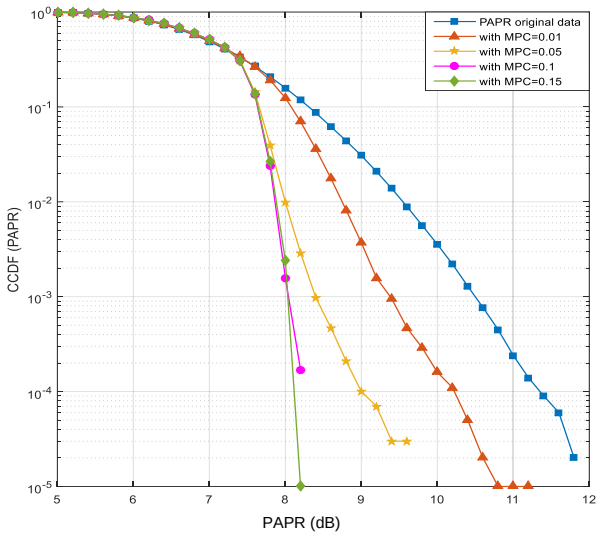

Figure 3.8 CCDF of proposed BR algorithm with different MPC values for 50×50 P-to-P massive MIMO-OFDM, PAPR target value = 5.5dB, using a combined search algorithm

3.3.3. Capacity analysis of proposed BR algorithm

Figure 3.9 and 3.10 show the capacity curves of our proposed BR algorithm for a 50×50 massive MIMO-OFDM system without and with water-filling, respectively. The figures and their closeup view show that the capacity loss due to our proposed algorithm is marginal.

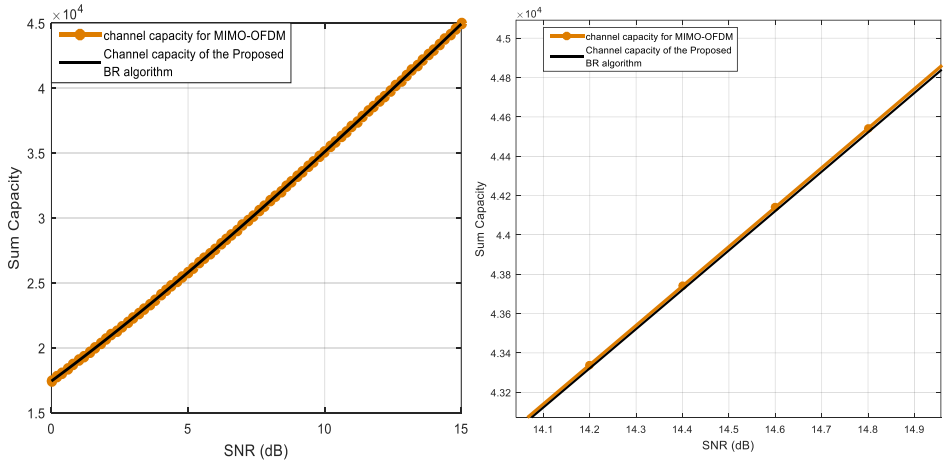

Figure 3.9 Channel capacity analysis for a P-to-P 50×50 massive MIMO-OFDM system utilizing BR algorithm

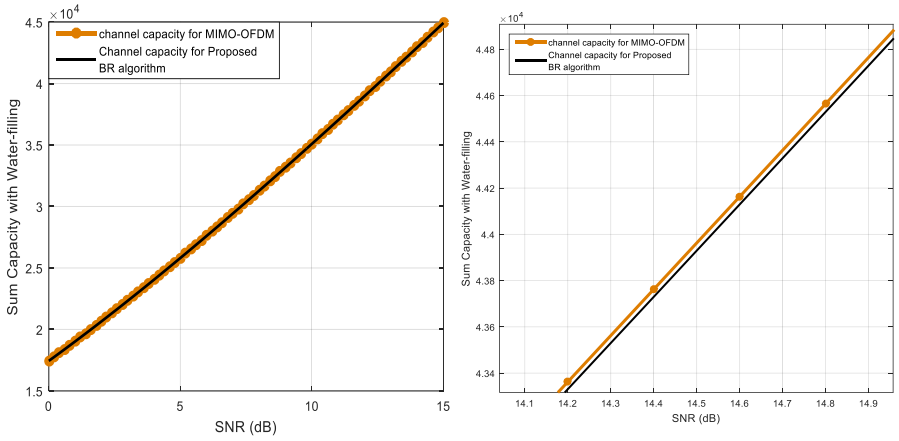

Figure 3.10 Channel capacity analysis for a P-to-P 50×50 massive MIMO-OFDM system utilizing BR algorithm with water-filling

3.4. Conventional TR vs Proposed BR algorithm

We compared different parameters between our proposed BR algorithm and conventional TR algorithm (CTR), to ascertain the performance level of our proposed solution.

3.4.1. PAPR reduction comparison

Fig 3.11 and 3.12 show the performance comparison of our BR algorithm with the conventional TR algorithm for 10×10 and 50×50 MIMO-OFDM systems, respectively. For the TR algorithm, the number of reserved tones is 10% and the number of iterations is 100. For a 10×10 MIMO-OFDM system a gain of 6.4dB is obtained with our proposed solution as compared to 4.4dB with CTR.

Moreover, for a 50×50 MIMO-OFDM system a gain of 4.8dB is obtained with our proposed BR algorithm as compared to a gain of 3.6dB with CTR. The simulation results thus show that our proposed BR algorithm outperforms the CTR by 2 dB (10×10) and 1.2 dB (50×50).

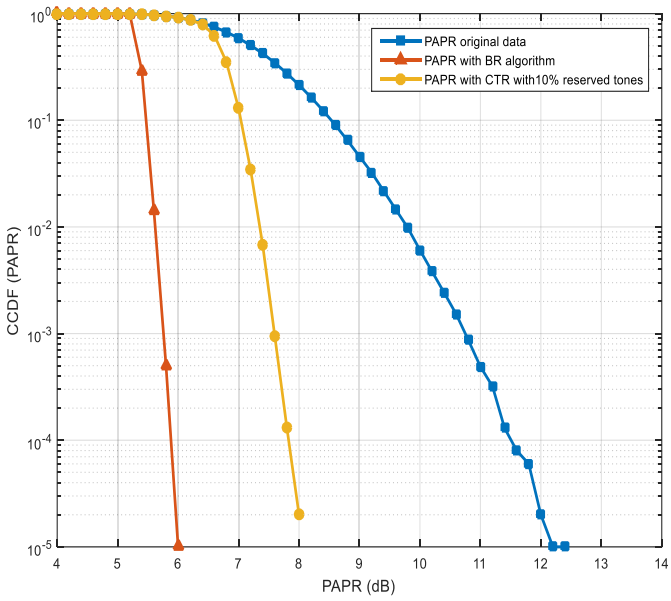

Figure 3.11 CCDF(PAPR) comparison of a 10×10 MIMO-OFDM system using BR (BR) with a system using CTR with 10% reserved tones

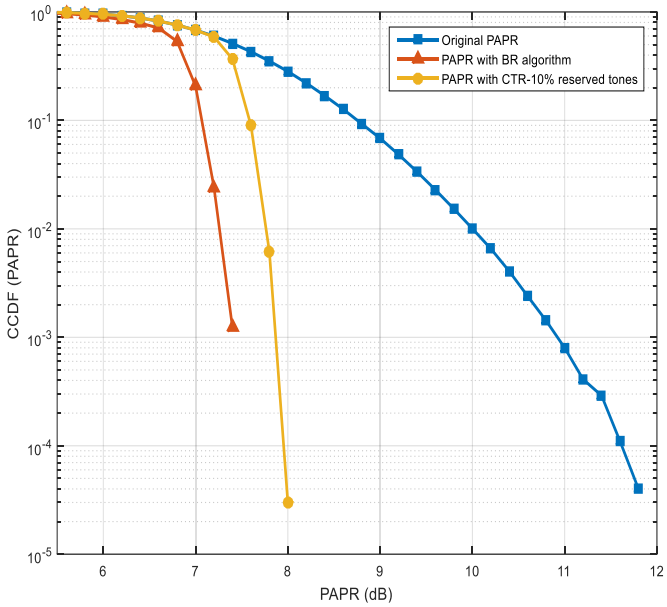

Figure 3.12 CCDF(PAPR) comparison of a 50×50 massive MIMO-OFDM system using BR with a system using CTR with 10% reserved tones

We can, therefore, deduce that the PAPR reduction by using our proposed method is much better than the conventional TR algorithm working with 10% reserved tones.

3.4.2. Performance comparison under mean power constraint

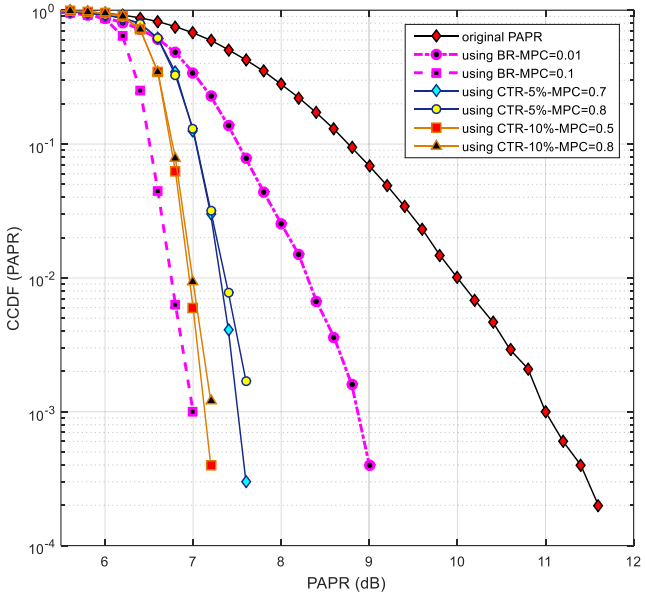

Figure 3.13 CCDF for a 10×10 P-to-P MIMO-OFDM system, using BR and CTR algorithms under a mean power constraint

Fig 3.13 shows the performance curve of the proposed BR with CTR under mean power constraint for a 10×10 MIMO-OFDM system. While using conventional TR with 5% and 10% reserved tones, the PAPR of the system reduces with an increase in ΔE value. The system with reserved tones at 10%, performs better than the system with reserved tones at 5%. Whereas, our proposed BR algorithm performs even better than the conventional TR, as the system using our algorithm gives a fast convergence with minimal increase in the mean transmit power.

3.4.3. Capacity loss of CTR against our proposed BR algorithm

Channel capacity of a MIMO-OFDM system utilizing the CTR [9] can be written as

$$\mathcal{C}_T = \sum_{N-\theta} \sum_{i=1}^{M} log_2 \left(1 + ð_i(n)\sigma_i^2(n)\right), \tag{3.18}$$

where $\sigma_i^2$is the singular value and $ð_i$ is the SNR.

Where as the channel capacity for the MIMO-OFDM system using our roposed BR algorithm is calculated as

$$\mathcal{C}_T = \sum_{N-\theta} \sum_{i=1}^{M-1} log_2 \left(1 + \mathrm{d}_i(n)\sigma_i^2(n)\right) \quad (3.19)$$

Here we will share the simulated results for channel capacity curves for a comparison between MIMO-OFDM using conventional TR (CTR) algorithm and our proposed BR algorithm.

We have simulated capacity curves for 10×10 and 50×50 MIMO-OFDM systems, with 128 sub-carriers using the original curves for MIMO-OFDM, the CTR with different percentages of reserved tones and our BR algorithm.

For 10×10 and 50×50 MIMO-OFDM systems, we will analyse the capacity loss of our Proposed BR algorithm against MIMO-OFDM using conventional TR algorithm and MIMO-OFDM without using any PAPR reduction algorithm, with and without water-filling.

10×10 P-to-P MIMO-OFDM Systems

Fig 3.14 and 3.15 show the capacity analysis for a 10×10 p-to-p MIMO-OFDM without and with water-filling, respectively. We observed that the capacity loss due to our proposed BR algorithm-based MIMO-OFDM system is much smaller than that of the conventional TR. The curves show that capacity loss due to our proposed solution is even smaller than 3% of the CTR.

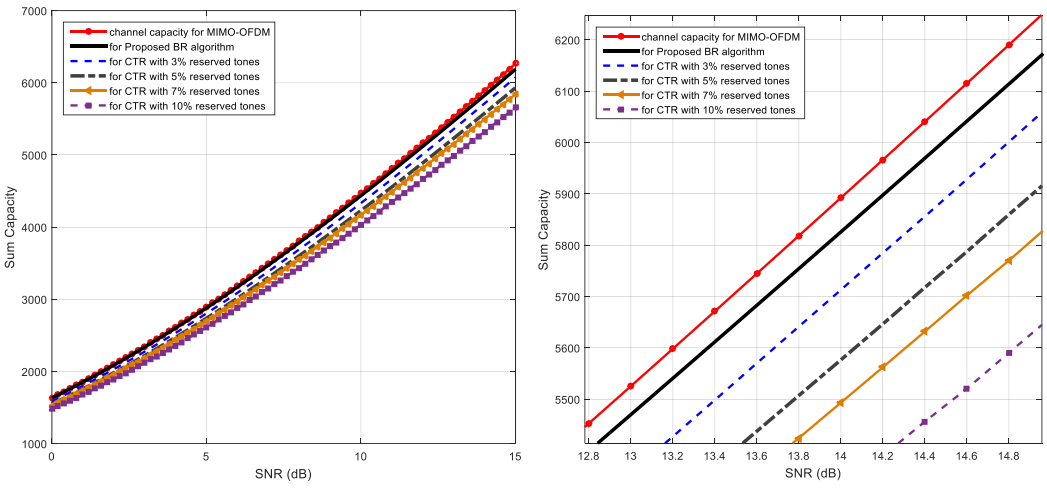

Figure 3.14 Capacity analysis for a P-to-P 10×10 MIMO-OFDM system utilizing BR with a system using CTR with different values of reserved tones

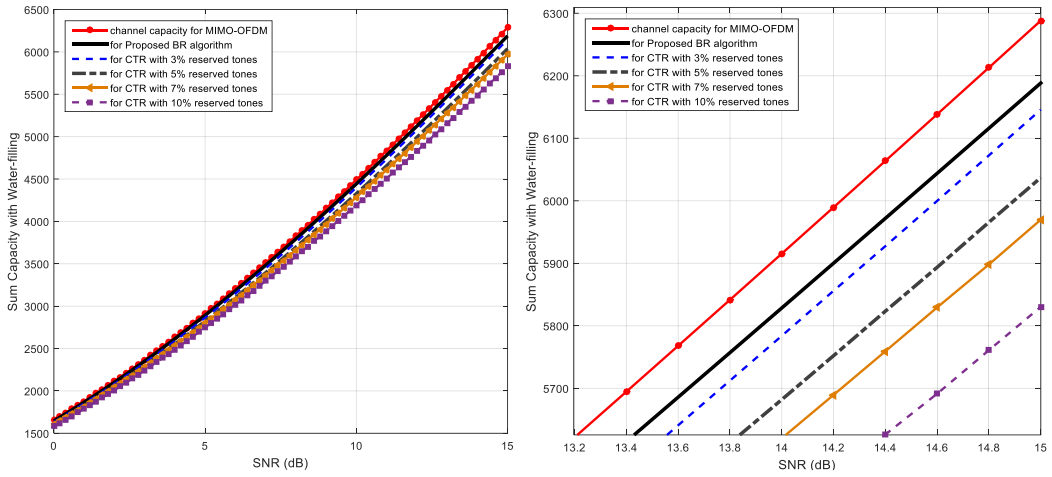

Figure 3.15 Capacity analysis for a P-to-P 10×10 MIMO-OFDM system utilizing BR with a system using CTR with different values of reserved tones with water-filling

50×50 P-to-P massive MIMO-OFDM Systems

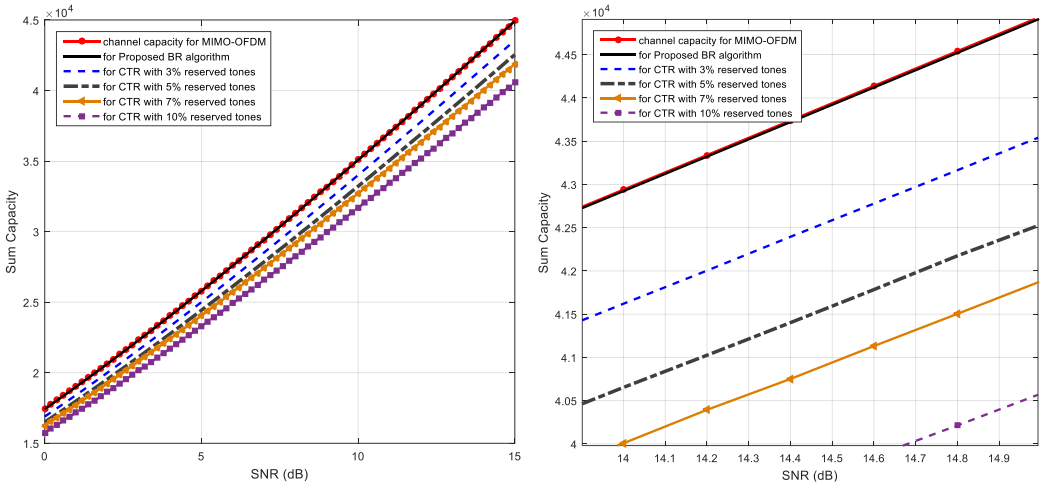

Figure 3.16 Capacity analysis for a P-to-P 50×50 massive MIMO-OFDM system utilizing BR with a system using CTR with different values of reserved tones

Fig 3.16 and 3.17 show the capacity analysis for a 50×50 p-to-p MIMO-OFDM without and with water-filling, respectively. We observed that the capacity loss due to our proposed BR algorithm-based MIMO-OFDM system is very much smaller than that of the conventional TR. The curves show that capacity loss due to our proposed solution is even smaller than 3% of the CTR.

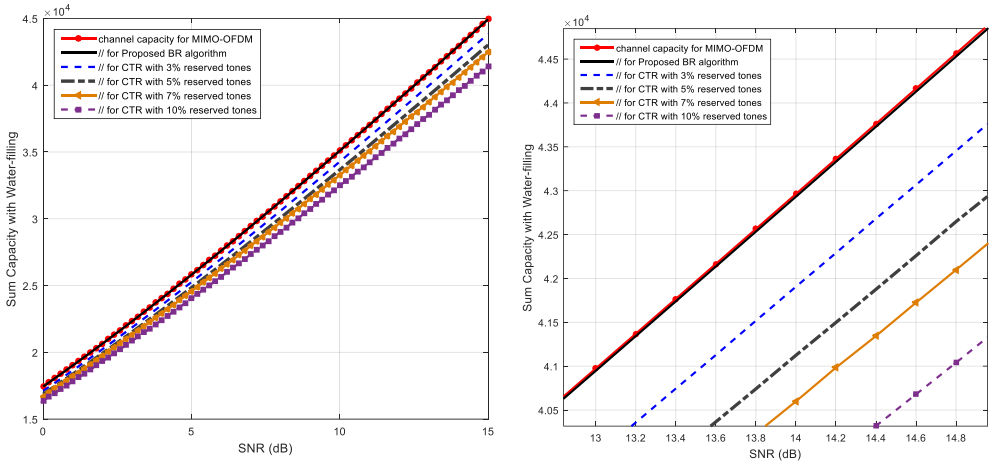

Figure 3.17 Capacity analysis for a P-to-P 50×50 massive MIMO-OFDM system utilizing BR with a system using CTR with different values of reserved tones with water-filling

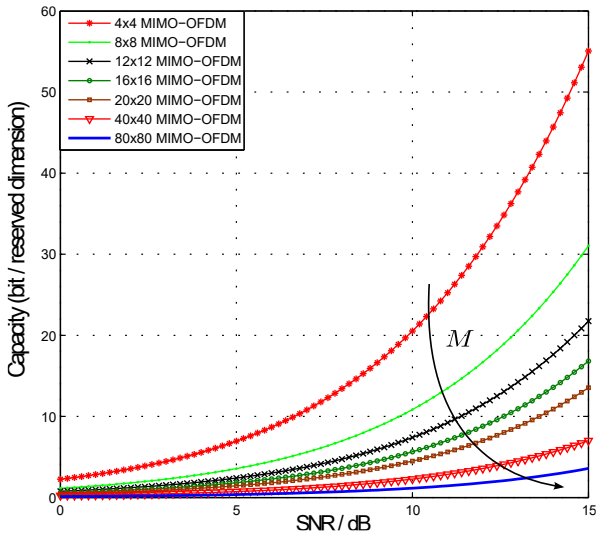

Figure 3.18 Capacity associated with last eigenchannel

Figure 3.18 shows the capacity curves associated with the last eigenchannel that is reserved for different MIMO-OFDM systems. From the above fig., it is observed that the capacity loss (due to reservation of weakest eigenchannel) decreases, with the increase in dimensionality of MIMO-OFDM system. The capacity loss due to the reserved dimension, for a 20×20 MIMO-OFDM system, is only 13 bits and as low as 4 bits for a 80 × 80 MIMO-OFDM systems.

It can be concluded that the capacity loss due to our proposed solution is smaller than the CTR algorithm and this loss diminishes as the number of antennas grows.

Chapter 4:
Conclusion

In this thesis, we proposed the Beam Reservation algorithm for PAPR reduction in P-to-P Massive MIMO-OFDM system. We designed a novel spiky function to be generated at the weakest eigen channel of our channel matrix, for PAPR redundancy as this channel is not suitable for data transmission.

The simulated results of our proposed BR algorithm are discussed in section 3.3. In section 3.4, we compared the performance of our proposed BR algorithm with the conventional TR algorithm using evaluating parameters like CCDF (PAPR), mean power increase and channel capacity. From section 3.4, it is clear that the proposed BR algorithm produces better results, i.e., PAPR reduction, fast convergence under mean power constraints and minimum capacity loss.

References

[1] R. W. Chang, ‘Synthesis of Band-Limited Orthogonal Signals for Multichannel Data Transmission’, *Bell Syst. Tech. J.*, vol. 45, no. 10, pp. 1775–1796, 1966.

[2] B. R. Saltzberg, ‘Performance of an Efficient Parallel Data Transmission System’, *IEEE Trans. Commun. Technol.*, vol. COM-15, no. 6, pp. 805–811, 1967.

[3] S. B. Weinstein and P. M. Ebert, ‘Data Transmission by Frequency-Division Multiplexing Using the Discrete Fourier Transform’, *IEEE Trans. Commun. Technol.*, vol. 19, no. 5, pp. 628–634, 1971.

[4] A. Oppenheim *et al.*, ‘Digital Signal Processing 24.0 Digital Signal Processing Academic and Research Staff Part-time Assistants/Special Projects’, 1999.

[5] A. Peled and A. Ruiz, ‘FREQUENCY DOMAIN DATA TRANSMISSION USING REDUCED COMPUTATIONAL COMPLEXITY ALGORITHMS.’, in *Record - IEEE International Conference on Acoustics, Speech & Signal Processing*, 1980, vol. 3, pp. 964–967.

[6] B. Hirosaki, ‘An Analysis of Automatic Equlizers for Orthogonally Multiplexed QAM Systems’, *IEEE Trans. Commun.*, vol. 28, no. 1, pp. 73–83, 1980.

[7] B. Hirosaki, ‘An Orthogonally Multiplexed QAM System Using the Discrete Fourier Transform’, *IEEE Trans. Commun.*, vol. 29, no. 7, pp. 982–989, 1981.

[8] R. Lassalle and M. Alard, ‘Principles of modulation and channel coding for digital broadcasting for mobile receivers’, *EBU Tech. Rev*, vol. 224, no. 1, pp. 68–190, 1987.

[9] A. Goldsmith, *Wireless communications*, vol. 9780521837163. Cambridge University Press, 2005.

[10] L. Hanzo, B. J. Choi, and T. Keller, ‘OFDM and MC-CDMA for Broadband Multi-user Communications, WLANs and Broadcasting’, 2005.

[11] C. E. Shannon, ‘A mathematical theory of communication’, *Bell Syst. Tech. J.*, vol. 27, no. 3, pp. 379–423, 1948.

[12] G. J. Foschini and M. J. Gans, ‘On Limits of Wireless Communications in a Fading Environment when Using Multiple Antennas’, *Wirel. Pers. Commun.*, vol. 6, no. 3, pp. 311–335, 1998.

[13] E. Telatar, ‘Capacity of multi-antenna Gaussian channels’, *Eur. Trans. Telecommun.*, vol. 10, no. 6, pp. 585–595, 1999.

[14] A. Paulraj, A. P. Rohit, R. Nabar, and D. Gore, *Introduction to space-time wireless communications*. Cambridge university press, 2003.

[15] H. Määttänen, ‘MIMO-OFDM’, *S-72.333 Postgrad. Course Radio Commun.*

[16] E. G. Larsson, O. Edfors, F. Tufvesson, and T. L. Marzetta, ‘Massive MIMO for next generation wireless systems’, *IEEE Commun. Mag.*, vol. 52, no. 2, pp. 186–195, 2014.

[17] C. Shepard *et al.*, ‘Argos: Practical many-antenna base stations’, in *Proceedings of the Annual International Conference on Mobile Computing and Networking, MOBICOM*, 2012, pp. 53–64.

[18] R. Van Nee and A. De Wild, ‘Reducing the peak-to-average power ratio of OFDM’, in *48th IEEE Vehicular Technology Conference. Pathway to Global Wireless Revolution*, 1998, vol. 3, pp. 2072–2076.

[19] A. Gangwar and M. Bhardwaj, ‘An overview: Peak to average power ratio in OFDM system & its effect’, *Int. J. Commun. Comput. Technol.*, vol. 1, no. 2, pp. 22–25, 2012.

[20] S. Hussain, ‘Peak to average power ratio analysis and reduction of cognitive radio signals’. Université Rennes 1, 2009.

[21] R. Gross and D. Veeneman, ‘SNR and spectral properties for a clipped DMT ADSL signal’, in *Proceedings of ICC/SUPERCOMM’94-1994 International Conference on Communications*, 1994, pp. 843–847.

[22] R. O’Neill and L. B. Lopes, ‘Envelope variations and spectral splatter in clipped multicarrier signals’, in *Proceedings of 6th International Symposium*

on Personal, Indoor and Mobile Radio Communications, 1995, vol. 1, pp. 71–75.

[23] D. J. G. Mestdagh and P. M. P. Spruyt, 'A method to reduce the probability of clipping in DMT-based transceivers', *IEEE Trans. Commun.*, vol. 44, no. 10, pp. 1234–1238, 1996.

[24] X. Li and L. J. Cimini, 'Effects of clipping and filtering on the performance of OFDM', in *1997 IEEE 47th Vehicular Technology Conference. Technology in Motion*, 1997, vol. 3, pp. 1634–1638.

[25] J. Armstrong, 'New OFDM peak-to-average power reduction scheme', in *IEEE Vehicular Technology Conference*, 2001, vol. 1, no. 53rd, pp. 756–760.

[26] J. Armstrong, 'Peak-to-average power reduction for OFDM by repeated clipping and frequency domain filtering', *Electron. Lett.*, vol. 38, no. 5, pp. 246–247, 2002.

[27] L. Wang and C. Tellambura, 'Clipping-noise guided sign-selection for PAR reduction in OFDM systems', *IEEE Trans. signal Process.*, vol. 56, no. 11, pp. 5644–5653, 2008.

[28] Y.-C. Wang and Z.-Q. Luo, 'Optimized iterative clipping and filtering for PAPR reduction of OFDM signals', *IEEE Trans. Commun.*, vol. 59, no. 1, pp. 33–37, 2010.

[29] R. W. Bauml, R. F. H. Fischer, and J. B. Huber, 'Reducing the peak-to-average power ratio of multicarrier modulation by selected mapping', *Electron. Lett.*, vol. 32, no. 22, pp. 2056–2057, 1996.

[30] S. H. Muller and J. B. Huber, 'OFDM with reduced peak-to-average power ratio by optimum combination of partial transmit sequences', *Electron. Lett.*, vol. 33, no. 5, pp. 368–369, 1997.

[31] S. H. Han and J. H. Lee, 'An overview of peak-to-average power ratio reduction techniques for multicarrier transmission', *IEEE Wireless Communications*, vol. 12, no. 2. pp. 56–65, Apr. 2005, doi: 10.1109/MWC.2005.1421929.

[32] S. H. Muller and J. B. Huber, ‘A comparison of peak power reduction schemes for OFDM’, in *GLOBECOM 97. IEEE Global Telecommunications Conference. Conference Record*, 1997, vol. 1, pp. 1–5.

[33] J. Tellado, ‘Peak-to-average power reduction for multicarrier modulation’, *Ph. D. thesis*, 1999.

[34] J. Tellado and J. M. Cioffi, ‘Peak power reduction for multicarrier transmission’, in *IEEE GLOBECOM*, 1998, vol. 99, pp. 5–9.

[35] Y.-L. Lee, Y.-H. You, W.-G. Jeon, J.-H. Paik, and H.-K. Song, ‘Peak-to-average power ratio in MIMO-OFDM systems using selective mapping’, *IEEE Commun. Lett.*, vol. 7, no. 12, pp. 575–577, 2003.

[36] M.-S. Baek, M.-J. Kim, Y.-H. You, and H.-K. Song, ‘Semi-blind channel estimation and PAR reduction for MIMO-OFDM system with multiple antennas’, *IEEE Trans. Broadcast.*, vol. 50, no. 4, pp. 414–424, 2004.

[37] H. Bao, J. Fang, Q. Wan, Z. Chen, and T. Jiang, ‘An ADMM Approach for PAPR Reduction for Large-Scale MIMO-OFDM Systems’, *IEEE Trans. Veh. Technol.*, vol. 67, no. 8, pp. 7407–7418, 2018, doi: 10.1109/TVT.2018.2837112.

[38] C. Siegl and R. F. H. Fischer, ‘Peak-to-average power ratio reduction in multi-user OFDM’, in *2007 IEEE International Symposium on Information Theory*, 2007, pp. 2746–2750.

[39] R. F. H. Fischer and M. Hoch, ‘Directed selected mapping for peak-to-average power ratio reduction in MIMO OFDM’, *Electron. Lett.*, vol. 42, no. 22, pp. 1289–1290, 2006.

[40] R. F. H. Fischer and M. Hoch, ‘Peak-to-average power ratio reduction in MIMO OFDM’, *IEEE Int. Conf. Commun.*, pp. 762–767, 2007, doi: 10.1109/ICC.2007.130.

[41] C. Siegl and R. F. H. Fischer, ‘Selected Sorting for PAR reduction in OFDM multi-user broadcast scenarios’, 2009.

[42] C. Siegl and R. F. H. Fischer, ‘Asymptotic performance analysis and

successive selected mapping for PAR reduction in OFDM', *IEEE Trans. Signal Process.*, vol. 58, no. 6, pp. 3228–3237, 2010.

[43] S. Umeda, 'Low-complexity PAPR reduction method for multiuser MIMO-OFDM systems with block diagonalization', in *Inter. OFDM-Workshop 2010, Sept.*, 2010, pp. 11–15.

[44] J. Gao, J. Wang, and Z. Xie, 'Peak to average power ratio reduction for MIMO-OFDMsystems with decomposed selected mapping', *Int. J. Inf. Syst. Sci.*, vol. 3, no. 3–4, pp. 572–580, 2009.

[45] B. Rihawi, Y. Louet, and S. Zabré, 'PAPR reduction scheme with SOCP for MIMO-OFDM', in *2007 International Conference on Wireless Communications, Networking and Mobile Computing*, 2007, pp. 271–274.

[46] A. Wakeel and W. Henkel, 'Least-squares iterative PAR reduction for point-to-point large-scale MIMO-OFDM systems', in *2014 IEEE International Conference on Communications (ICC)*, 2014, pp. 4638–4643.

[47] S. Umeda, S. Suyama, H. Suzuki, and K. Fukawa, 'PAPR reduction method for block diagonalization in multiuser MIMO-OFDM systems', *IEEE Veh. Technol. Conf.*, pp. 1–5, 2010, doi: 10.1109/VETECS.2010.5493834.

[48] T. Liu, L. Ni, S. Jin, and X. You, 'Angular domain precoding-based PAPR reduction for massive MIMO systems', *Sci. China Inf. Sci.*, vol. 62, no. 10, pp. 222–226, 2019, doi: 10.1007/s11432-019-9805-9.

[49] H. Bao, J. Fang, Q. Wan, Z. Chen, and T. Jiang, 'An ADMM Approach for PAPR Reduction for Large-Scale MIMO-OFDM Systems', *IEEE Trans. Veh. Technol.*, vol. 67, no. 8, pp. 7407–7418, 2018, doi: 10.1109/TVT.2018.2837112.

[50] T. Kageyama, O. Muta, C. M. Chen, and S. Pollin, 'Effect of Limiter Based PAPR Reduction for Massive MIMO Systems', *2018 Proc. Japan-Africa Conf. Electron. Commun. Comput. JAC-ECC 2018*, no. 1, pp. 43–46, 2019, doi: 10.1109/JEC-ECC.2018.8679567.

[51] T. Kageyama and O. Muta, 'Bit error rate analysis of mrc precoded massive MIMO-OFDM systems with peak cancellation', *IEEE Veh. Technol. Conf.*,

vol. 2019-Septe, pp. 12–17, 2019, doi: 10.1109/VTCFall.2019.8891444.

[52] A. Ivanov, A. Volokhatyi, D. Lakontsev, and D. Yarotsky, ‘Unused Beam Reservation for PAPR Reduction in Massive MIMO System’, *IEEE Veh. Technol. Conf.*, vol. 2018-June, pp. 1–5, 2018, doi: 10.1109/VTCSpring.2018.8417537.

[53] M. Yao *et al.*, ‘Semidefinite Relaxation-Based PAPR-Aware Precoding for Massive MIMO-OFDM Systems’, vol. 68, no. 3, pp. 2229–2243, 2019.

[54] T. Kageyama, O. Muta, and H. Gacanin, ‘Enhanced Peak Cancellation with Simplified In-Band Distortion Compensation for Massive MIMO-OFDM’, *IEEE Access*, vol. 8, pp. 73420–73431, 2020, doi: 10.1109/ACCESS.2020.2986280.

[55] C. A. Schmidt, M. Crussière, J. F. Hélard, and A. M. Tonello, ‘Improving energy efficiency in massive MIMO: Joint digital beam-steering and tonereservation PAPR reduction’, *IET Commun.*, vol. 14, no. 14, pp. 2250–2258, 2020.

[56] A. Kalinov, R. Bychkov, A. Ivanov, A. Osinsky, and D. Yarotsky, ‘Machine Learning-Assisted PAPR Reduction in Massive MIMO’, *IEEE Wirel. Commun. Lett.*, vol. 10, no. 3, pp. 537–541, 2021, doi: 10.1109/LWC.2020.3036909.

[57] A. Ivanov and D. Lakontsev, ‘Selective tone reservation for PAPR reduction in wireless communication systems’, in *2017 IEEE International Workshop on Signal Processing Systems (SiPS)*, 2017, pp. 1–6.